

# **Stony Brook University**



OFFICIAL COPY

**The official electronic file of this thesis or dissertation is maintained by the University Libraries on behalf of The Graduate School at Stony Brook University.**

**© All Rights Reserved by Author.**

**Fluoride as a Probe for Hydrogen-bonding in the Distal Heme Pocket of Tt H-NOX**

A Thesis Presented

By

**John Kosowicz**

To

The Graduate School

In Partial Fulfillment of the

Requirements

for the Degree of

**Master of Science**

In

**Chemistry**

Stony Brook University

**May 2012**

Copyright by  
John G. Kosowicz  
2012

**Stony Brook University**

The Graduate School

**John Kosowicz**

We, the thesis committee for the above candidate for the  
Master of Science degree, hereby recommend  
acceptance of this thesis.

**Elizabeth M. Boon, Ph.D., Thesis Advisor**

Professor, Department of Chemistry

**Daniel P. Raleigh, Ph.D., Committee Chair**

Professor, Department of Chemistry

**Dale G. Drueckhammer, Ph.D., Third Member**

Professor, Department of Chemistry

This thesis is accepted by the Graduate School

Charles Taber

Interim Dean of the Graduate School

Abstract of the Thesis

**Fluoride as a Probe for Hydrogen-bonding in the Distal Heme Pocket of *Tt* H-NOX**

By

**John Kosowicz**

**Master of Science**

in

**Chemistry**

Stony Brook University

**2012**

Probing the hydrogen bonding environment in the heme pocket of a hemoprotein can greatly aid in understanding ligand specificity in hemoproteins. For example, soluble guanylate cyclase (sGC), a eukaryotic nitric oxide (NO) sensor, has picomolar sensitivity to NO, while completely excluding molecular oxygen (O<sub>2</sub>) as a ligand. The current hypothesis to explain this ligand specificity is that sGC lacks distal pocket hydrogen bond donors that would preferentially stabilize O<sub>2</sub> as a ligand. Interestingly, a closely related bacterial homolog of sGC, the H-NOX (Heme-Nitric oxide/OXygen binding) domain from *Thermoanaerobacter tengcongensis* (*Tt*) binds O<sub>2</sub> with a dissociation constant of 90nM. Structural studies of *Tt* H-NOX indicate that there are three distal pocket residues that form a hydrogen bonding network that may stabilize O<sub>2</sub> binding. This work focuses on characterizing the distal heme pocket hydrogen-bonding network in *Tt* H-NOX. Previous studies have shown that the wavelength maximum of the charge-transfer band (CT1) in the electronic spectrum of a fluoride-heme complex is a sensitive probe of distal pocket hydrogen-bonding. Using this assay, we found that tyrosine 140 (Y140) in the distal pocket of *Tt* H-NOX donates the strongest hydrogen bonding to bound fluoride.

Additionally, we found that mutation of phenylalanine 78 (F78) to tyrosine (F78Y) donates an additional hydrogen bond to bound fluoride. We also observe that tryptophan 9 (W9) and asparagine 74 (N74) play a role in the stabilization of Y140. In the W9F, N74A and W9F/N74A mutants, Y140 has a weaker hydrogen-bond with fluoride. However, the stabilization of Y140 by W9 appears to be very low. N74 provides the majority of hydrogen-bond stabilization to Y140, indicating that W9 may have evolved to fulfill some other evolutionary need.

The structure of the heme cofactor is critical for hemoprotein function. These functions include transportation and storage of diatomic gases, chemical catalysis, diatomic gas detection, and electron transfer. In *Tt* H-NOX WT, the heme has been shown to be distorted, due to a proline in the 115 position. In order to investigate the nature of the non-planar heme in H-NOX, we created a panel of mutant *Tt* H-NOX proteins, in which the proline in position 115 was mutated to various residues (P115G, P115A, P115L, P115V, P115W and P115F). At the conclusion of this work we were unable to find a link between heme planarity and redox potential or ligand stabilization by hydrogen-bonding. However, we are undertaking further studies to reach this goal.

## Table of Contents

|   |      |
|---|------|
| List of figures.....  | vii  |
| List of tables.....   | viii |
| Abbreviations.....  | ix   |
| Chapter 1. Background.....  | 1    |
| 1.1 H-NOX.....  | 1    |
| 1.2 <i>Thermoanaerobacter tengcongensis</i> H-NOX.....  | 3    |
| 1.3 Heme deformation in <i>Thermoanaerobacter tengcongensis</i> H-NOX.....                                  | 4    |
| 1.4 Heme Pocket of <i>Thermoanaerobacter tengcongensis</i> H-NOX.....                                       | 5    |
| 1.5 UV-VIS spectroscopy.....  | 7    |
| 1.6 Fluoride as a Heme Pocket Probe.....  | 9    |
| 1.7 Oxidation-Reduction Potentiometry.....  | 10   |
| Chapter 2. Fluoride as a Probe for Hydrogen-bonding in the Distal Heme Pocket of <i>Tt</i> H-NOX...11       |      |
| 2.1 Abstract.....   | 11   |
| 2.2 Introduction.....   | 13   |
| 2.3 The Heme Pocket in <i>Tt</i> H-NOX.....   | 14   |
| 2.4 The Charge-transfer (CT1) band in <i>Tt</i> H-NOX.....  | 15   |
| 2.5 Materials and Methods.....  | 16   |
| 2.6 Results and Discussion.....   | 20   |
| 2.7 Conclusions.....  | 34   |
| Chapter 3. Investigations into the relationship between heme planarity and function in <i>Tt</i> H-NOX..... | 35   |

|                                 |    |
|---------------------------------|----|
| 3.1 Abstract.....               | 35 |
| 3.2 Introduction.....           | 36 |
| 3.3 Materials and Methods.....  | 38 |
| 3.4 Results and Discussion..... | 40 |
| 3.5 Conclusions.....            | 48 |
| References.....                 | 49 |
| Appendix A.....                 | 51 |
| Appendix B.....                 | 55 |



## List of Figures

|  |    |
|--|----|
| 1-1 <i>Tt</i> H-NOX Crystal Structure.....   | 2  |
| 1-2 <i>Tt</i> H-NOX WT and P115A Heme Overlay.....                                   | 4  |
| 1-3 <i>Tt</i> H-NOX WT Heme Pocket.....  | 6  |
| 1-4 <i>Tt</i> H-NOX UV-VIS Spectra.....  | 8  |
| 2-1 CT1 Band Spectra of <i>Tt</i> WT and mutants.....                                | 20 |
| 2-2 $K_D$ Titrations for <i>Tt</i> WT and mutants.....                               | 22 |
| 2-3 Decreasing hydrogen-bond strength decreases the CT1 band absorbance maximum..... | 33 |
| 3-1 Redox pontentiometry set-up.....   | 39 |
| 3-2 CT1 band measurements of <i>Tt</i> H-NOX WT and P115X mutants.....               | 43 |
| 3-3 Redox titrations of <i>Tt</i> H-NOX WT and P115X mutants.....                    | 45 |

## List of Tables

|  |    |
|--|----|
| 2-1 Primers for site-directed mutagenesis.....   | 18 |
| 2-2 CT1 band absorbance maximum, $K_{D(F^-)}$ titrations for <i>Tt</i> H-NOX WT and mutants.....                   | 23 |
| 3-1 Measurements of CT1 band absorbance maximum and redox titrations for <i>Tt</i> H-NOX WT and P115X mutants..... | 42 |

## Abbreviations

sGC - soluble guanylate cyclase

O<sub>2</sub> - molecular oxygen

NO - nitric oxide

*Tt* - *Thermoanaerobacter tengcongensis*

H-NOX - Heme-Nitric oxide/OXygen binding domain

CT1 - charge-transfer band (600-620 nm)

XAFS - x-ray absorption fine structure

SHE – Standard Hydrogen Electrode

## Chapter 1: Background Information

### 1.1 H-NOX

The Heme Nitric Oxide and/or OXygen binding (H-NOX) domain family is a family of hemoprotein sensors conserved from bacteria to man (1). The H-NOX domain contains a histidine-ligated ferrous protoporphyrin IX heme and has evolved to bind nitric oxide (NO) and/or diatomic oxygen (O<sub>2</sub>). Soluble guanylate cyclase (sGC), present in mammals, contains an H-NOX domain and has been shown to be involved in vasodilation (2). Several bacterial homologs have been structurally and biochemically investigated. While the function of bacterial H-NOX domains are not well understood, studies suggest they function as NO sensors to regulate cellular responses such as biofilm formation (3, 4) and quorum sensing (5).

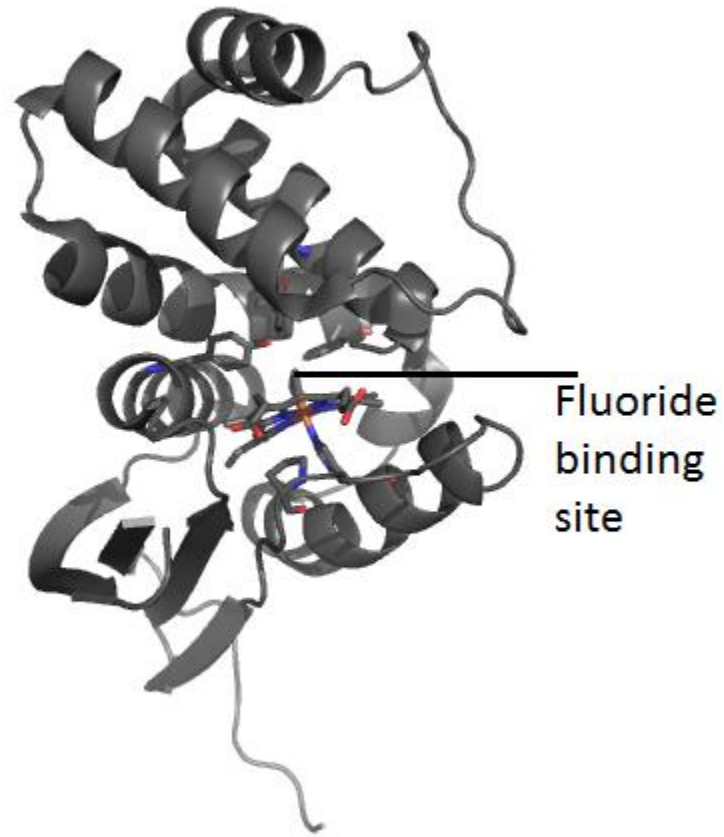


Figure 1-1. *Tt* H-NOX crystal structure (PDB 1U55). (6)

## 1.2 *Thermoanaerobacter tengcongensis* H-NOX

A particularly well-studied bacterial H-NOX domain is that from *Thermoanaerobacter tengcongensis* (6). *Thermoanaerobacter tengcongensis* (*Tt*) is an anaerobic, thermophilic bacterium obtained from hot springs in Tengcong, China (7). Likely due to its native organism, *Tt* H-NOX is easily overexpressed and purified from standard *E. coli* expression systems and it is extremely stable. Because of these properties, as well as its homology to sGC, *Tt* H-NOX is a good model for H-NOX characterization (6).

*Tt* H-NOX is a 188 amino-acid heme protein that can bind diatomic gaseous molecules such as NO, O<sub>2</sub>, CO and other anionic small molecules (8). *Tt* H-NOX has been shown to bind diatomic oxygen (O<sub>2</sub>) in the Fe<sup>2+</sup> state, whereas eukaryotic proteins (sGC) do not bind diatomic oxygen (9).

### 1.3 Heme deformation in *Tt* H-NOX

Crystal structures of *Tt* H-NOX have demonstrated that the heme cofactor is extremely distorted from planarity (6, 10). A proline in the distal pocket (P115 in *Tt* H-NOX) is responsible for this heme conformation (11, 12). Mutation of the proline in position 115 to alanine causes the heme to become more relaxed and planar (11). Our group has recently shown that heme flattening is sufficient for signal transduction in the H-NOX family (8).

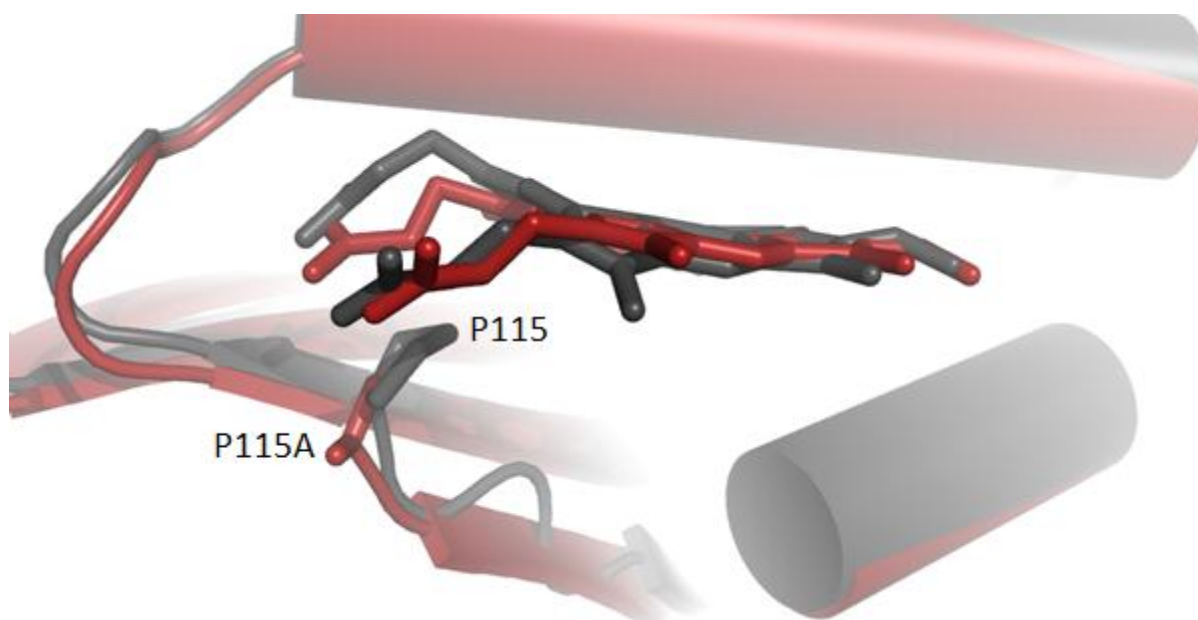


Figure 1-2. *Tt* H-NOX WT (PDB 1U55) overlaid with *Tt* H-NOX P115A (PDB 3EEE). *Tt* H-NOX WT is grey; *Tt* H-NOX P115A is red. Figure generated in Pymol.

#### **1.4 Heme Pocket of *Thermoanaerobacter tengcongensis* H-NOX**

The heme pocket of *Tt* H-NOX is sterically crowded, and binding characteristics have been related to steric crowding in the distal heme pocket (13). The proximal heme pocket contains a heme-bound histidine in position 102 (9). The distal heme pocket contains a tyrosine in position 140, which has been shown to donate an important hydrogen bond to bound diatomic oxygen (Figure 1-3). Additionally, a tryptophan in position 9 and an asparagine in position 74 are thought to stabilize tyrosine 140. These residues are not present in aerobic H-NOX proteins such as sGC, explaining why aerobic H-NOX domains tend to exclude O<sub>2</sub> as a ligand (14). Finally, a phenylalanine in position 78 is ideally positioned to be mutated to a tyrosine, which could then donate a hydrogen bond to a bound anion (15).



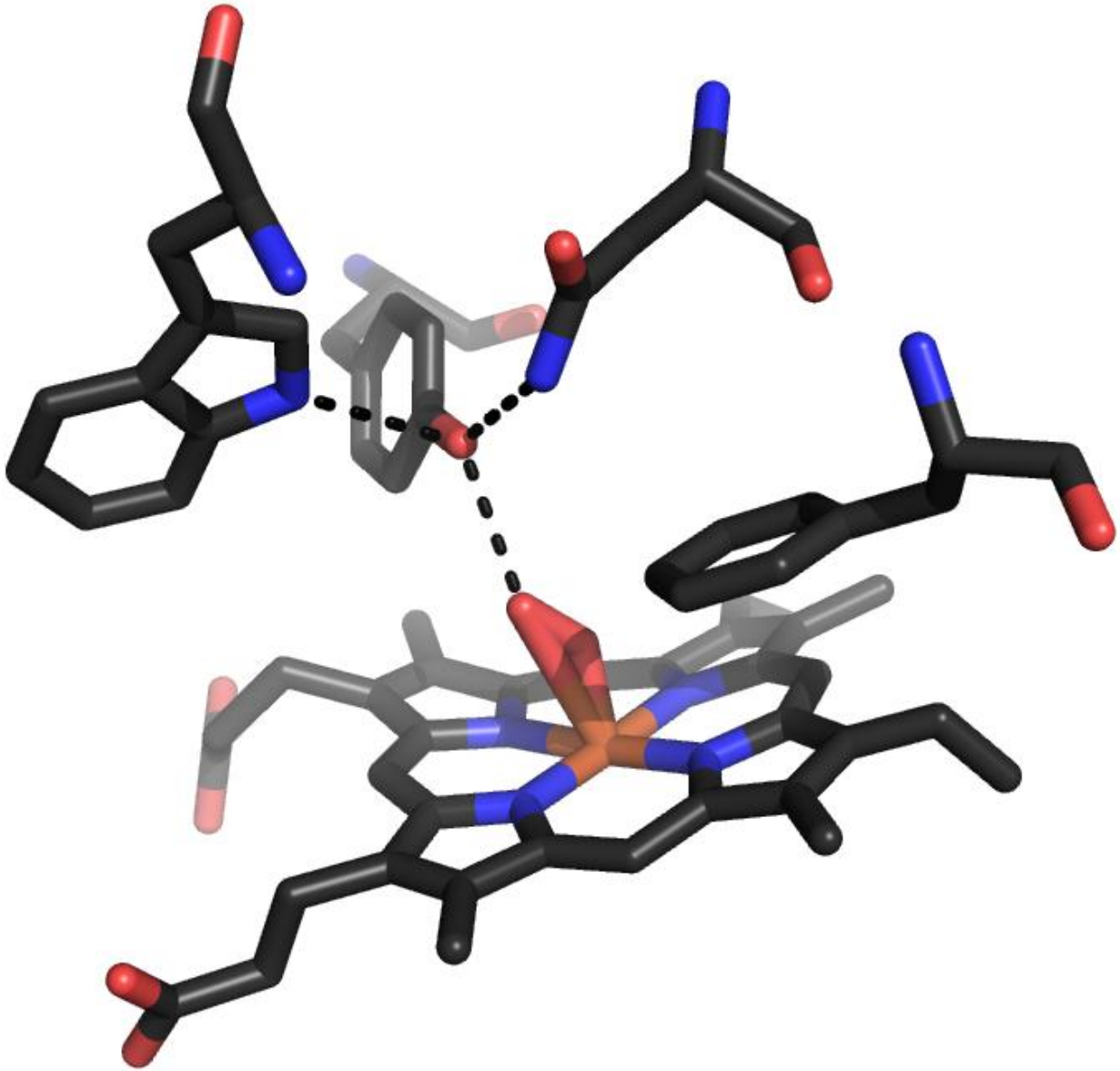


Figure 1-3. A view of the residues involved in hydrogen bond stabilization of bound ligand in *Tt* H-NOX. From left to right: W9, Y140, N74 and F78. Adapted from (6); figure generated in Pymol.

## 1.5 UV-VIS Spectroscopy

UV-VIS spectroscopy is a valuable tool for measuring the general electronic properties as well as the ligand-binding properties of heme proteins. Heme proteins have a high extinction absorbance called the Soret band that is sensitive to the ligation and oxidation state of the heme cofactor (16). Therefore, the UV-VIS spectra of a heme protein can be used to examine what types of ligands are bound to the heme, to assess the level of hemoprotein purity (comparison of the absorbance of the Soret band to the absorbance at 280 nm), and to measure the protein concentration. Because ligand to heme binding causes a change in the absorbance of the Soret band, one can measure association and dissociation rate constants using electronic spectroscopy.

The region between 500 nm and 600 nm of the spectra of *Tt* H-NOX contains the  $\alpha/\beta$  bands. The  $\alpha/\beta$  bands can be used as an indicator for ligand binding (13).

The wavelength of maximum of the charge-transfer (CT1) band of heme proteins is sensitive to the heme pocket environment (17). This band is affected by vinyl conjugation to the porphyrin macrocycle and the axial ligand fields. In general, a decrease of the field increases the energy of the  $e_g(d_g)$  orbitals resulting in an increase of frequency and intensity of the CT1 band. The energy of the  $(d_g)$  orbitals of the heme iron is affected by interactions with the p and  $\pi$  orbitals of the axial ligand. In particular, H-bonding with water molecules or residues in the heme cavity affects the nature of the ligand p orbital interaction with the iron orbitals, and this the wavelength maximum of the CT1 band. Fluoride binds in the distal heme pocket to heme

iron, and this has been previously shown to be a good probe of hydrogen-bonding when used in conjunction with the CT1 band (17).

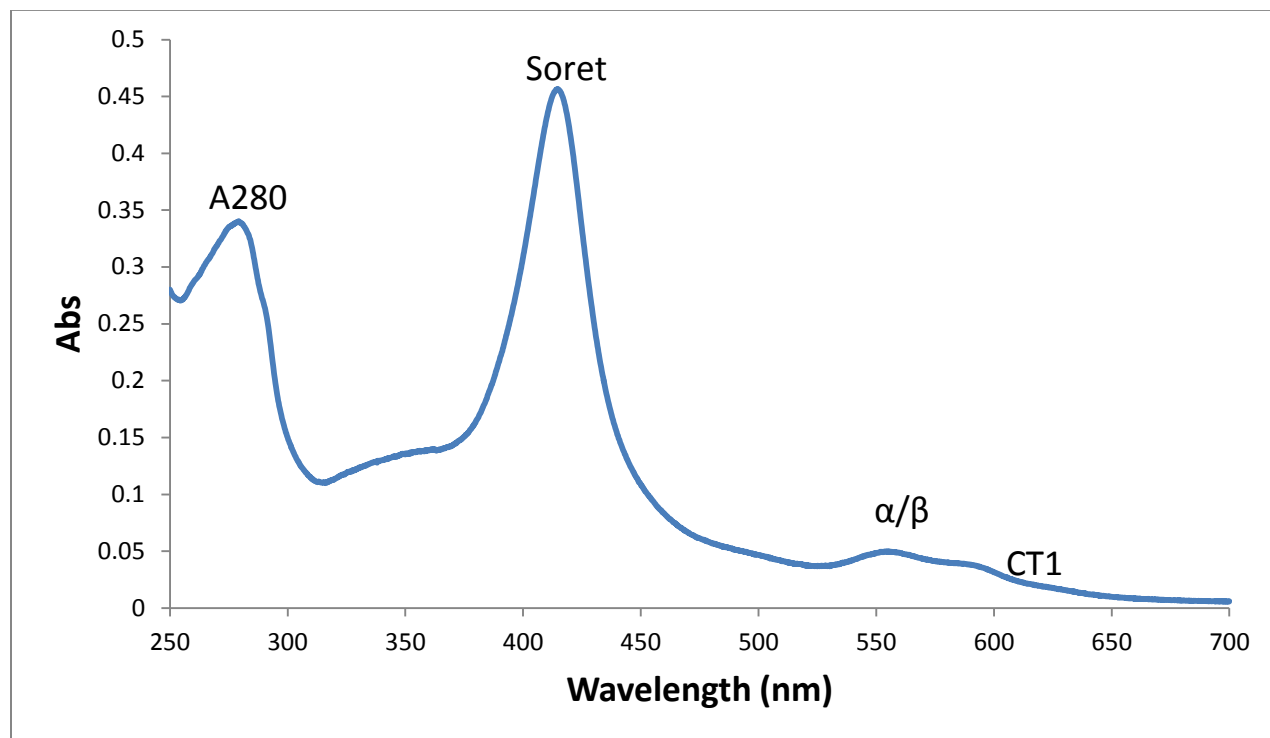


Figure 1-4. Typical *Tt* H-NOX UV-VIS spectra.

## 1.6 Fluoride as a Heme Pocket Probe

Previous studies have shown that the CT1 band of a fluoride-heme complex is a particularly sensitive probe of the hydrogen-bonding environment in the distal heme cavity of heme proteins (17). An increase in hydrogen-bonding to the bound fluoride ligand decreases the availability of the fluoride p and  $\pi$  orbitals for interaction with the heme p and  $\pi$  orbitals. This causes the p and  $\pi$  orbitals of the heme iron to go to a lower energy state, which results in a red shift in the CT1 band maximum (17). Conversely, a decrease in hydrogen-bonding to the bound fluoride ligand increases the energy of the heme p and  $\pi$  orbitals, causing an increase in the strength of the Fe-F bond, and a blue shift in the CT1 wavelength maximum. Resonance Raman (RR) studies have confirmed that the aforementioned red shift is due to the weakening of the Fe-F bond and that the blue shift is due to the strengthening of the Fe-F bond (17).

## 1.7 Oxidation-reduction Potentiometry

Oxidation-reduction (redox) potentiometry is a tool that has applications towards understanding the energetics and chemistry involved with electron transfer processes in hemoproteins. The data provided by redox potentiometry can be used to help determine characteristics of hemoprotein redox reactions. Measuring the redox potential of a hemoprotein is an easy process, and can be done with a pH meter and a spectrophotometer (12).

In combination with UV-VIS spectroscopy, one can measure the midpoint potentials of heme proteins simply by tracking the changes in spectra versus the standard hydrogen electrode (SHE) potential measurements. Using a reducing agent, one can reduce a protein to a more negatively charged state, which can be measured. Because *Tt* H-NOX contains a heme, it is possible to use redox potentiometry to measure what effect mutants have on the heme center in terms of their redox potential. The  $\text{Fe}^{3+}$  and  $\text{Fe}^{2+}$  states of heme iron in *Tt* H-NOX have different Soret spectra. Therefore, it is possible to measure at what potential vs. SHE the heme is half reduced, which would be its midpoint potential.

## Chapter 2: Fluoride as a Probe for Hydrogen-bonding in the Distal Heme Pocket of *Tt* H-NOX

### 2.1 Abstract

Probing the hydrogen bonding environment in the heme pocket of a hemoprotein can greatly aid in understanding ligand specificity in hemoproteins. For example, soluble guanylate cyclase (sGC), a eukaryotic nitric oxide (NO) sensor, has picomolar sensitivity to NO, while completely excluding molecular oxygen (O<sub>2</sub>) as a ligand. The current hypothesis to explain this ligand specificity is that sGC lacks distal pocket hydrogen bond donors that would preferentially stabilize O<sub>2</sub> as a ligand. Interestingly, a closely related bacterial homolog of sGC, the H-NOX (Heme-Nitric oxide/OXygen binding) domain from *Thermoanaerobacter tengcongensis* (*Tt*) binds O<sub>2</sub> with a dissociation constant of 90nM. Structural studies of *Tt* H-NOX indicate that there are three distal pocket residues that form a hydrogen bonding network that may stabilize O<sub>2</sub> binding. This work focuses on characterizing the distal heme pocket hydrogen-bonding network in *Tt* H-NOX. Previous studies have shown that the wavelength maximum of the charge-transfer band (CT1) in the electronic spectrum of a fluoride-heme complex is a sensitive probe of distal pocket hydrogen-bonding. Using this assay, we found that tyrosine 140 (Y140) in the distal pocket of *Tt* H-NOX donates the strongest hydrogen bonding to bound fluoride. Additionally, we found that mutation of phenylalanine 78 (F78) to tyrosine (F78Y) donates an additional hydrogen bond to bound fluoride. We also observe that tryptophan 9 (W9) and asparagine 74 (N74) play a role in the stabilization of Y140. In the W9F, N74A and W9F/N74A mutants, Y140 has a weaker hydrogen-bond with fluoride. However, the stabilization of Y140 by W9 appears to be very low. N74 provides the majority of hydrogen-bond stabilization to Y140, indicating that W9 may have evolved to fulfill some other evolutionary need.



## 2.2 Introduction

The environment in the heme pockets of heme proteins plays an important role in determining ligand specificity and affinity. It has been suggested in *Thermoanaerobacter tengcongensis* (*Tt*) H-NOX (Heme Nitrogen and/or Oxygen binding domain) that a distal pocket hydrogen-bonding network regulates ligand specificity and affinity. Mutation of certain residues involved in hydrogen-bonding in the distal heme pocket disrupted the position of tyrosine 140 (Y140), causing the protein to lose binding of diatomic oxygen (O<sub>2</sub>) (15). Additionally, it has been shown that rational mutation of distal pocket residues can tune the affinity of *Tt* H-NOX for ligands in both the ferrous and ferric oxidation states (13, 14). Given this, it is of importance to quantify the contribution to the strength of the hydrogen-bonding network of each residue in the distal heme pocket of *Tt* H-NOX.

Previous studies using truncated myoglobins and a series of commercially available hemoproteins (peroxidases) have shown that fluoride can be used in conjunction with a charge-transfer band in the UV-VIS spectrum around 610 nm (the “CT1” band) to characterize the hydrogen bonding environment the distal pocket of hemoproteins. The more the bound fluoride is stabilized by hydrogen-bonding, the more red-shifted the CT1 band will be; the less the bound fluoride is stabilized by hydrogen-bonding, the more blue shifted the CT1 band will be (17).



### **2.3 The Heme Pocket in *Tt* H-NOX**

*Tt* H-NOX has been extensively studied. X-ray crystal structures reveal that the distal heme pocket contains a tyrosine 140 (Y140), which is positioned to donate a hydrogen bond to heme-bound ligands. Additionally, tryptophan 9 (W9) and asparagine 74 (N74) are thought to stabilize Y140 through hydrogen-bonding, thus forming a distal pocket hydrogen-bonding network. Finally, phenylalanine 78 (F78) is directed towards the distal coordination site such that if mutated to tyrosine (F78Y), it could also donate a hydrogen bond to a bound ligand (15).

## 2.4 The charge-transfer (CT1) band in *Tt* H-NOX

The wavelength maximum of the CT1 band in a hemoprotein such as *Tt* H-NOX is sensitive to polarity of the bound ligand and whether or not the bound ligand is forming hydrogen-bonds with distal pocket residues (17). When the bound ligand is only weakly (or not) serving as a hydrogen-bond acceptor, the ligand has more p and/or  $\pi$  orbitals available, which when interacting with the heme iron, increase the heme iron p and  $\pi$  orbital energy. This causes a blue shift in the CT1 band. The CT1 band will red shift when the ligand is strongly interacting with distal pocket residues through acceptance of hydrogen-bonds. Stabilizing the ligand with additional hydrogen-bonds makes the ligands p and  $\pi$  orbitals less available for interaction with the heme iron p and  $\pi$  orbitals. This causes the p and  $\pi$  orbitals of the heme iron to go into a lower energy state, which results in a red shift in the CT1 band maximum (17).

We hypothesize that the CT1 band in the UV-VIS spectra of *Tt* H-NOX will display a correlation to the strength of hydrogen bonds donated to fluoride and that we can characterize hydrogen bonding in the distal heme pocket by mutating residues to manipulate the level of hydrogen bond stabilization of the bound fluoride. The absorbance maximum of the CT1 band occurs at 609 nm in wild-type (WT) *Tt* H-NOX. Removing hydrogen-bonds from the ligand should result in a stronger Fe-F bond, which would blue-shift the CT1 band maximum. Conversely, adding H-bonding residues should weaken the Fe-F bond, resulting in a red-shifted CT1 band.

## 2.5 Materials and Methods

Mutagenesis, protein expression, purification and storage

*Tt* H-NOX wild-type (WT) was previously cloned into the pET 20(b) vector in-frame with a C-terminal hexa-histidine tag (6xHis-tag) (18). Mutations were then made to this inserted gene.

Mutagenic primers were designed according to QuikChange (Stratagene) guidelines (Table 1).

*Tt* H-NOX mutants were prepared using the QuikChange Protocol (Stratagene). Mutant plasmids (containing ampicillin resistance) were transformed into DH5 $\alpha$  (no antibiotic resistance) *E. coli* cells and selected on ampicillin-containing Bacto-agar plates (1.5% agar, 100 $\mu$ g/mL ampicillin). The ampicillin resistance gene in the pET 20(b) vector ensures that only cells that took up the plasmid would survive and reproduce on the ampicillin plates. Colonies were then grown overnight in LB media at 37°C with agitation at 250rpm, and the mutant plasmids were purified using Zymo Mini-Prep kits. Purified plasmids were subsequently submitted for sequencing to confirm mutation. Once confirmed through sequencing, the mutant plasmids were transformed into Tuner DE3(pLysS) *E. coli* cells (chloramphenicol resistant), plated on ampicillin and chloramphenicol-containing plates (1.5% agar, 100 $\mu$ g/mL ampicillin, 12.5 $\mu$ g/mL). The double resistance ensures that only TunerDE3(pLysS) cells that take up the plasmid survive and reproduce. The proteins were expressed in yeast extract media (after a growth period of ~4 hours at 37°C with agitation at 250rpm) at 18°C with agitation at 250rpm for 16 hours. Protein expression was induced using a final concentration of 10 $\mu$ M IPTG

(Isopropyl  $\beta$ -D-1-thiogalactopyranoside). After expression, the media was centrifuged at 7,000rpm for 10 minutes at 4°C to harvest the cells. The cell pellet was resuspended in lysis buffer (300mM NaCl, 50mM sodium phosphate dibasic, pH 7.5). The cells were lysed by sonication (30% output, 1-second pulse time, on-and-off for one minute at a time on ice for 40 minutes). After lysis and centrifugation at 18,000rpm for 30 minutes at 4°C to remove cell membranes and debris, the soluble cell supernatant was heated to 75°C for 15 minutes (*Tt* H-NOX is native to a thermophilic organism and thus it is heat stable) to denature contaminating *E. coli* proteins. This heat-denatured solution was then centrifuged at 18,000rpm for 30 minutes at 4°C and the supernatant was run over Ni-NTA agarose beads (nickel affinity) that had been equilibrated with buffer (300mM sodium chloride, 50mM sodium phosphate dibasic, pH 7.5). Because *Tt* H-NOX is 6xHis-tagged, it is prevented from flowing through the column through ligation to the immobilized Ni-NTA in the column matrix. *Tt* H-NOX-bound beads were washed with 300mM NaCl, 50mM sodium phosphate dibasic buffer containing 10, 20 and 30mM imidazole (pH 7.5) to elute contaminants. The purified protein was eluted using 300mM NaCl, 50mM sodium phosphate dibasic buffer containing 250mM imidazole (pH 7.5). Imidazole and other buffer salts were partially removed and the protein was concentrated using Millipore 3,000 MW spin-columns (Amicon) by centrifugation at 5000xg at 4°C for 15 minutes per spin. The concentrated protein was diluted 10x in 50mM HEPES, 50mM NaCl buffer (pH = 7.5). This process was repeated 5 times to ensure an imidazole concentration of no more than 2.5  $\mu$ M in the final protein aliquots. Proteins were stored in 50mM HEPES, 50mM NaCl (pH 7.5), 5% glycerol at -80°C for no more than two weeks prior to their use.

## Primer Design

| Mutation | Direction | Sequence  |
|----------|-----------|---|
| W9F      | Forward   | 5'-CAATCGTCGGGACATTCATAAAGACCCTAGGG-3'            |
| W9F      | Reverse   | 5'-CCCTCAGGGTCTTTATGAATGTCCCGACGATTG-3'           |
| Y140L    | Forward   | 5'-CTAAAAGAAAGATGTACGATCTTTTTTTAGGGCTTATAGAGGG-3' |
| Y140L    | Reverse   | 5'-CCCTCTATAAGCCCTAAAAAAGATCGTACATCTTTCTTTTAG-3'  |
| N74A     | Forward   | 5'-GAGAGGTAGGAAGGCAGGCGATAAAAACTTTCAGCG-3'        |
| N74A     | Reverse   | 5'-CGCTGAAAGTTTTTATCGCCTGCCTTCTACCTCTC-3'         |
| F78Y     | Forward   | 5'-GCAGAACATAAAAACTTACAGCGAATGGTTTCCC-3'          |
| F78Y     | Reverse   | 5'-GGGAAACCATTGCTGTAAGTTTTTATGTTCTGC-3'           |

Table 2-1. Primer sequences used for site-directed mutagenesis.

### Sample preparation

*Tt* H-NOX samples were thawed to room temperature and oxidized to their Fe<sup>3+</sup> complexes using 20mM potassium ferricyanide for one hour. Using a PD-10 column (GE Healthcare), the proteins were desalted to remove excess potassium ferricyanide as well as the ferrocyanide generated during H-NOX oxidation. The oxidized protein concentration was determined using the Soret band and appropriate extinction coefficient (100,000 M<sup>-1</sup>cm<sup>-1</sup>). Samples used to generate titration curves used for  $K_D$  determination and CT1 band measurements contained between 4 and 5  $\mu$ M protein (heme concentration). Potassium fluoride (KF) stock solutions (3M and 1M) were made by dissolving KF in 50mM HEPES, 50mM NaCl, pH 7.5. Serial dilutions of this concentrated stock solution were prepared by dilution into 50mM HEPES, 50mM NaCl, pH 7.5. Samples for spectroscopy were prepared by diluting purified

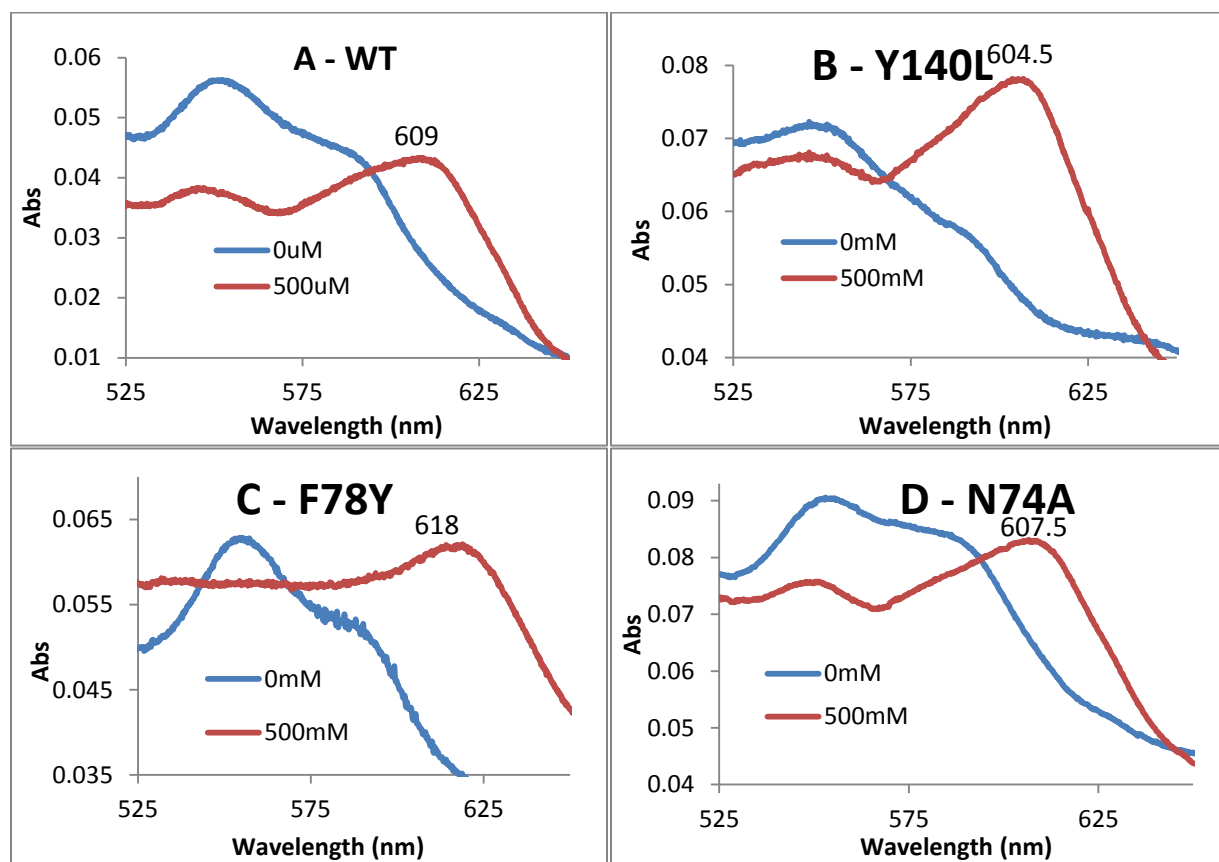
protein and KF in 50mM HEPES, 50 mM NaCl, pH 7.5 to the desired concentrations. *Tt* H-NOX was incubated with KF at ~22° C for four hours before UV/VIS measurements (Cary Bio 100) were taken.

Prior to scanning, the spectrophotometer was blanked using 50mM HEPES, 50mM NaCl, pH 7.5. The same cuvette was used for every measurement. Measurements were taken from 700 nm to 250 nm, with a step size of 0.2 nm.

## 2.6 Results and Discussion

### Electronic spectroscopy of the Fe<sup>3+</sup>-F complexes of *Tt* H-NOX WT and distal pocket mutants

The electronic spectroscopy of *Tt* H-NOX WT and mutants in the Fe<sup>3+</sup>-F complex were obtained and analyzed. The data are summarized in figure 2-1 and table 2-2.



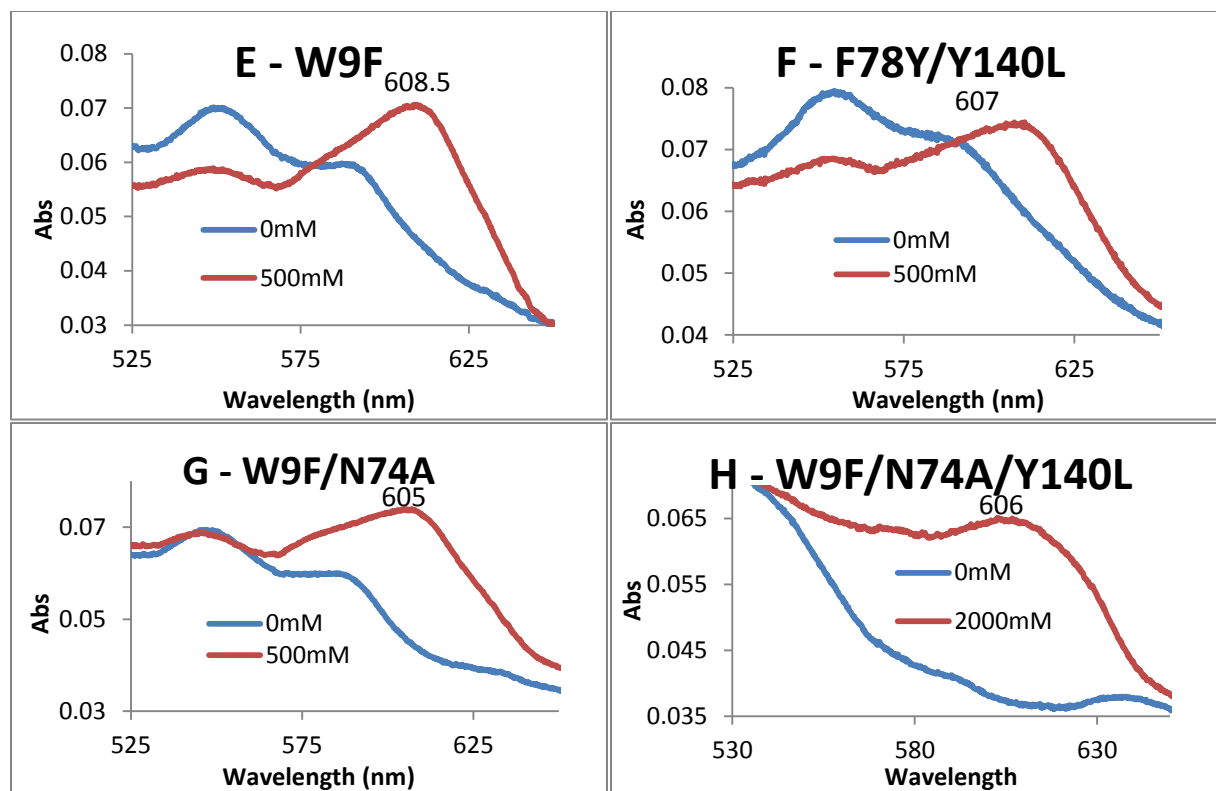
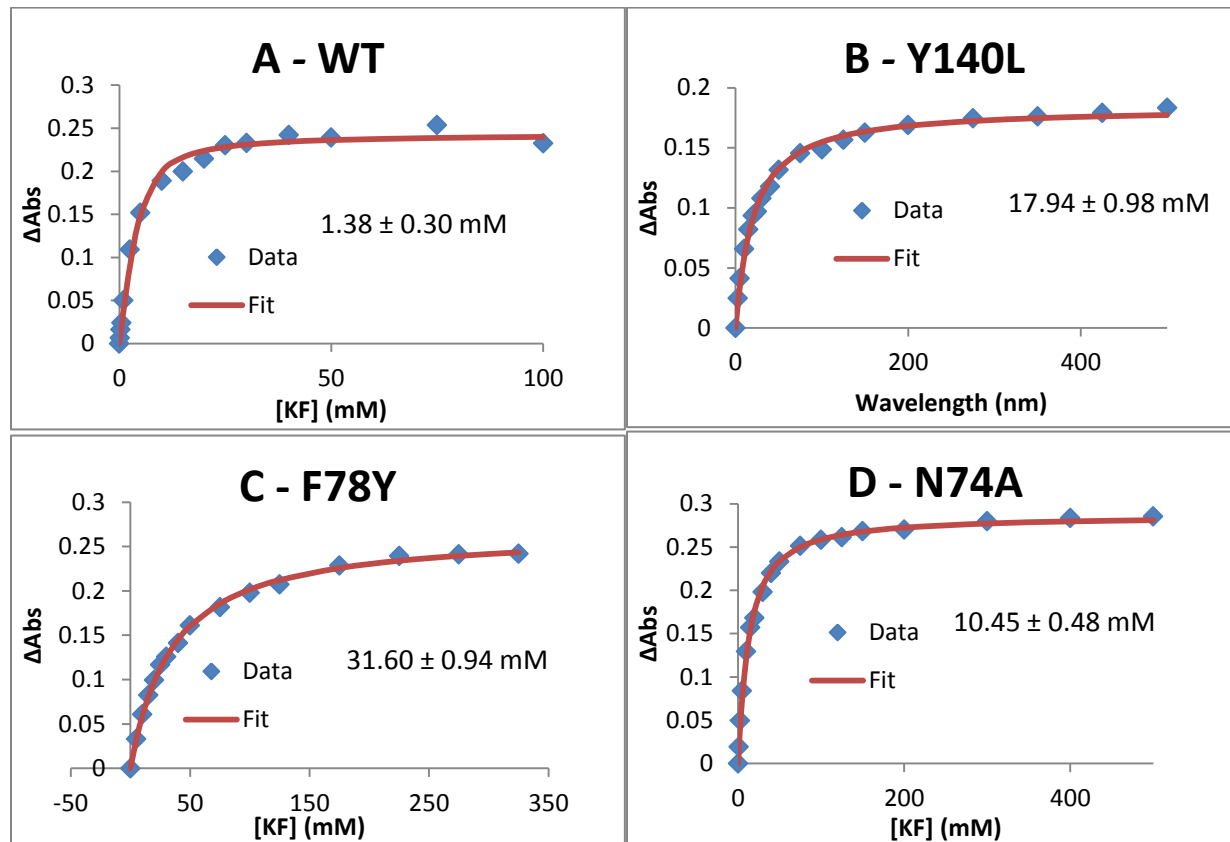


Figure 2-1. *Tt* H-NOX mutants 0 vs 500 (A-G) and 2000 (H) mM KF. A) *Tt* WT 0 vs. 500 mM KF. B) *Tt* Y140L 0 vs. 500mM KF. C) *Tt* F78Y 0 vs. 500mM KF. D) *Tt* H-NOX N74A 0 vs. 500mM KF. E) *Tt* W9F 0 vs. 500mM KF. F) *Tt* F78Y/Y140L 0 vs. 500mM KF. G) *Tt* H-NOX W9F/N74A 0 vs. 500 mM KF. H) *Tt* W9F/N74A/Y140L 0 vs. 2000mM KF.





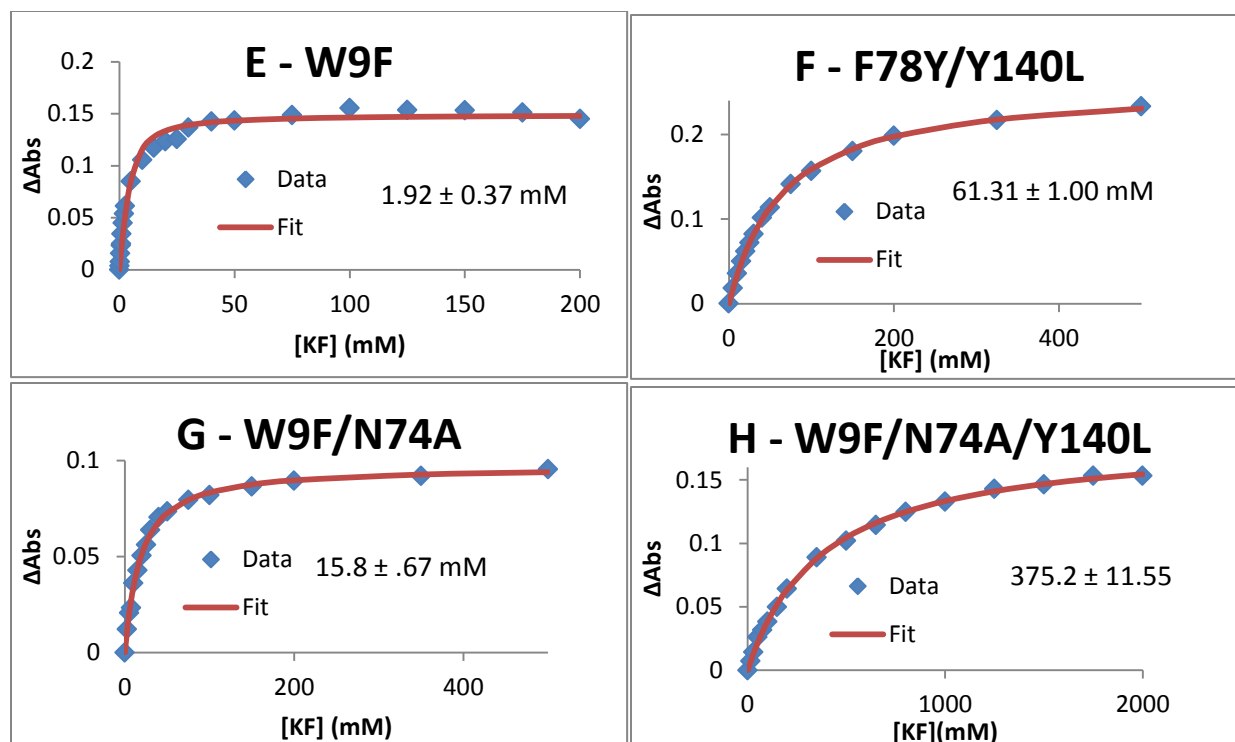


Figure 2-2. *Tt* H-NOX WT and mutants  $K_{D(F^-)}$  measurements. A) WT;  $1.38 \pm 0.30$  mM. B) Y140L;  $17.94 \pm 0.98$  mM. C) F78Y;  $31.60 \pm 0.94$  mM. D) N74A;  $10.45 \pm 0.48$  mM. E) W9F;  $1.92 \pm 0.37$  mM. F) F78Y/Y140L;  $61.31 \pm 1.00$  mM. G) W9F/N74A;  $15.8 \pm .67$  mM. H) W9F/N74A/Y140L;  $375.2 \pm 11.55$ .  $\Delta$ Abs on the Y axis refers to the change in absorbance as potassium fluoride is added. The data is processed by normalizing to 700 nm and 0 mM KF. The absorbance of the band indicating the  $Fe^{3+}$ -H<sub>2</sub>O state from each sample is subtracted from the increase in absorbance as measured by the band corresponding to the  $Fe^{3+}$ -F<sup>-</sup> state in each sample, giving a measurement of species change. The measurement of species change is then plotted against concentration of potassium fluoride in each sample. Errors were generated by averaging data.

| Protein         | CT1 absorbance band<br>maximum (nm) | $K_D$ (mM)      |
|-----------------|-------------------------------------|-----------------|
| <i>Tt</i> WT    | 609                                 | $1.47 \pm 0.16$ |
| <i>Tt</i> Y140L | 604.5                               | $18.2 \pm 1.6$  |
| <i>Tt</i> F78Y  | 618                                 | $32.4 \pm 0.70$ |
| <i>Tt</i> N74A  | 607.5                               | $9.96 \pm 0.49$ |

|                          |       |             |
|--------------------------|-------|-------------|
| <i>Tt</i> W9F            | 608.5 | 2.15 ± 0.04 |
| <i>Tt</i> F78Y/Y140L     | 607   | 57.2 ± 4.10 |
| <i>Tt</i> W9F/N74A       | 605   | 15.9 ± 0.67 |
| <i>Tt</i> W9F/Y140L/N74A | 606   | 375 ± 34.0  |

Table 2-2. *Tt* WT and mutants CT1 absorbance band maximum and  $K_{D(F^-)}$  measurements. See figures 1-1 and 1-2 for corresponding graphical representation. Errors were generated by averaging triplicate data.

### ***Tt* WT**

Using the CT1 maximum of *Tt* WT (609 nm) as a baseline, we can measure the hydrogen-bond strength donated to bound fluoride by the difference of the CT1 maximum of the mutants with respect to that of WT. The  $K_{D(F^-)}$  measurement of *Tt* WT ( $1.47 \pm 0.16$  mM) can also be used as a baseline, since the difference in the level of hydrogen-bond stabilization and  $K_{D(F^-)}$  measurements should be correlated.

### ***Tt* Y140L**

Tyrosine 140 is expected to provide the strongest hydrogen-bond to bound fluoride. Removal of this hydrogen-bond in the Y140L mutant resulted in a CT1 band maximum of 604.5 nm, which is 4.5 nm less than that of wild-type, confirming the strength of this hydrogen-bond. This matches our hypothesis – that a decrease in hydrogen-bond stabilization would result in an increase in the strength of the Fe-F bond, which is where the CT1 band is derived from, resulting in a blue-shifted CT1 band. Additionally, the  $K_{D(F^-)}$  of the Y140L mutant was measured to be  $18.24 \pm 1.59$  mM, which is a large difference from WT. This measurement is in line with the difference in hydrogen-bond stabilization. If the fluoride is not being stabilized by any

hydrogen bonds, it should not bind as tightly, even if the Fe-F bond is stronger in the Y140L mutant than in WT.

### **Tt F78Y**

F78 is directed towards the heme iron, and when mutated to tyrosine (F78Y), could donate an additional hydrogen bond to fluoride. The addition of an extra hydrogen bond is expected to weaken the Fe-F bond and result in a red-shifted CT1 band. We tested this theory by adding an additional hydrogen bond with the F78Y mutant. This mutation resulted in a CT1 band maximum of 618 nm, confirming the weakening of the Fe-F bond. This finding confirms that the hydroxyl of the tyrosine is donating a hydrogen bond to fluoride. Both Y140 and F78Y donating hydrogen bonds to fluoride yields a large red shift of the CT1 band. We also found that the  $K_{D(F^-)}$  is considerably higher than that of WT, measured at  $32.37 \pm 0.7$  mM. Our data from the Y140L, N74A and W9F mutant suggest an increase in the  $K_{D(F^-)}$  corresponds to a lack of hydrogen-bond stabilization of bound fluoride. Therefore, we were expecting to see a decrease in the  $K_{D(F^-)}$  with increasing hydrogen-bond stabilization of fluoride, to one lower than that of WT. We believe that in aside from adding hydrogen-bond stabilization to bound fluoride, sterics may play a role in causing the  $K_{D(F^-)}$  increase. Binding affinity ( $K_{D(F^-)}$ ) studies previously done have shown that the F78Y mutant introduces steric forces that inhibit fluoride binding vs. the F78V mutant (2). The length from the F78 residue to diatomic oxygen in the crystal structure is approximately 3.2 angstroms (6). Mutating F78 to F78Y adds a hydroxyl group. This hydroxyl group is large enough to be close to the fluoride binding site to slightly block it from binding, or

otherwise disrupt either N74 or Y140. This could account for the increased  $K_{D(F^-)}$  of the F78Y mutant.

### **Tt N74A**

N74 is expected to act as a hydrogen-bond stabilizer for Y140, which then donates the principal hydrogen bond to bound anionic ligands. Mutating N74 to N74A removes this stabilizing hydrogen bond, which then destabilizes the Y140-fluoride hydrogen-bond. This has the effect of lessening the amount of hydrogen-bond stabilization to fluoride, thereby strengthening the Fe-F bond and causing a blue shift in the CT1 maximum. The N74A mutant shows a CT1 band maximum of 607.5nm (in between Y140L and WT). This agrees with the Y140L and WT observations, because although Y140 is destabilized, it could still act as at least a partially stabilizing residue. Furthermore, the  $K_{D(F^-)}$  was measured to be  $9.96 \pm 0.49$  mM, which is also in between Y140L and WT, corresponding to a loss of hydrogen-bond stabilization.

### **Tt W9F**

W9 is believed to be involved in the stabilization of the Y140 hydrogen-bonding to fluoride, but it may have evolved to serve other functions. Based on our findings, we believe that W9 does not play a large role in the stabilization of Y140 with fluoride binds. The CT1 band maximum of the W9F mutant was measured to be 608.5 nm, which is very close to WT (609nm). The slight difference (0.5nm) could be due to some stabilization of Y140 by W9, but it is minimal at best. Additionally, the  $K_{D(F^-)}$  was measured to be  $2.15 \pm 0.04$  mM, which is also close to WT ( $1.47 \pm 0.16$  mM). Taken together, this suggests that the hydrogen-bonding

environment in the W9F mutant is similar to WT. We therefore believe that W9 does not play a large role in the hydrogen-bond stabilization of fluoride in the  $\text{Fe}^{3+}$  state of *Tt* H-NOX.

It has been shown in previous work that the distal heme hydrogen-bonding environment is tuned for  $\text{O}_2$  sensing and the ability to distinguish between  $\text{O}_2$  and NO. Additionally, it has been reported that W9 is important for the stabilization of Y140, which stabilizes bound  $\text{O}_2$ , and presumably in our assay, bound fluoride. Reported data indicate a factor of one-to-three decrease in  $\text{O}_2$  binding affinity characteristics, as illustrated by  $K_D$ ,  $k_{\text{on}}$ , and  $k_{\text{off}}$  in the  $\text{Fe}^{2+}$  state of the *Tt* H-NOX Y140L mutant vs. WT (14). Our data suggest that the W9F mutation does not greatly affect fluoride binding in the  $\text{Fe}^{3+}$  state of *Tt* H-NOX (Table 2).

These results may be attributable to several factors. First, fluoride is much smaller than diatomic oxygen. This size difference may have some effect on the ligand-bound protein. Since fluoride is an unnatural ligand, unintended changes may occur upon fluoride binding that do not occur when diatomic oxygen or nitric oxide binds. Another possibility is that W9 may have evolved to fulfill some role other than the stabilization of Y140, and it does nothing to stabilize Y140 when fluoride binds. It could also be that W9 has evolved to act as something in addition to being a stabilizer of Y140. In this case, it is entirely possible that W9 stabilizes Y140, but not as much as N74. CT1 band measurements of the N74A mutant show a CT1 band absorbance maximum at 607.5 nm. With the CT1 band at 608.5 in the W9F mutant, it appears that Y140 is only slightly stabilizing Y140, because a 0.5 nm shift corresponds to a comparatively small shift in the amount of hydrogen-bond stabilization afforded to bound fluoride. However, the W9F/N74A double mutant displays a CT1 absorbance maximum at 605 nm. This is interesting

because given the data from the W9F mutant one would expect the W9F/N74A double mutant to have properties similar to the N74A single mutant. This result supports the conclusions reached in previous studies, which demonstrate that mutating W9 to W9F causes an appreciable change in the binding characteristics of O<sub>2</sub> to *Tt* H-NOX in its ferrous form (14). Therefore, W9 may be involved in the stabilization of O<sub>2</sub>, but not fluoride.

### ***Tt* F78Y/Y140L**

Because Y140 has been shown to donate the principal hydrogen bond to bound ligand, and because F78 is ideally positioned to be mutated to a tyrosine which would then donate a hydrogen bond to fluoride, we decided to make the F78Y/Y140L mutant. We expected that if F78 is well enough positioned, mutating it to tyrosine might rescue the hydrogen bond stabilization provided to fluoride by Y140 in WT. The F78Y/Y140L mutant is less thermodynamically stable than any of the other mutants described here, but the CT1 band maximum was measured to be 607nm. This measurement falls in line with our other measurements. Y140 has probably evolved as the main stabilizing residue because it is most ideally suited for such work. Additionally, although by looking at the crystal structure of *Tt* H-NOX it appears that the F78Y mutant is well positioned to donate a hydrogen bond to fluoride, more effects than just the hydrogen bonding environment of the distal pocket can be affected when making mutations. Sterics, as mentioned earlier, may be playing a role in the high  $K_{D(F^-)}$  measurement in this mutant. Taking measurements into account, the F78Y mutant does not look quite as good as a possible hydrogen-bond donor. The additional hydroxyl group of the F78Y mutant could be creating steric clashes or interacting with hydrophobic residues in a

disruptive way. While F78Y makes up for some of the lost stabilization of fluoride by providing a hydrogen bond, it does not appear to stabilize fluoride and weaken the Fe-F bond as much as Y140 does. Because the F78Y/Y140L mutant does not express well and is not stable, it is not surprising that the  $K_{D(F^-)}$  is not in line with the  $K_{D(F^-)}$  of the other mutants. We measured the  $K_{D(F^-)}$  to be  $57.18 \pm 4.14$  mM. Like the F78Y mutant, sterics may be disrupting the heme pocket and be partly responsible for the high  $K_{D(F^-)}$ . The tyrosine in position 78 may be causing steric clashes as previously mentioned (F78Y section), and when combined with the lack of hydrogen-bond stabilization usually afforded to fluoride by Y140, a high  $K_{D(F^-)}$  seems reasonable.

#### ***Tt* W9F/N74A**

Since N74 has been shown to stabilize Y140 hydrogen-bonding to fluoride, and W9 might stabilize Y140 slightly, we hypothesize that mutating both of these residues to non-stabilizing residues would destabilize Y140, thereby destabilizing fluoride by keeping it from being preferentially stabilized by Y140. We also wanted to see whether or not the W9F/N74A displayed properties similar to the N74A mutant, which would confirm that W9 is not playing a large stabilizing role with respect to Y140. This mutation should increase the Fe-F bond strength, which would appear as a blue shift in the CT1 band maximum. The CT1 band maximum of the W9F/N74A mutant was measured to be 605nm (Y140L is 604.5nm, N74A is 607.5nm, W9F is 608.5nm, and WT is 609nm). This result is interesting because it could mean that although normally W9 does not play a particularly large role in stabilizing Y140, when N74 is mutated to N74A, maybe W9 plays a greater role in the stabilization of Y140. The CT1 band being blue-shifted with respect to the N74A mutant suggests that W9 could be a “back-up”



hydrogen-bond donor to Y140. The  $K_{D(F^-)}$  for the W9F/N74A mutant was measured to be  $15.85 \pm 0.67$  mM, which is in between the Y140L and N74A mutant. This result agrees with the type of hydrogen-bonding that is hypothesized to occur in this mutant, which is similar to the Y140L mutant.

### ***Tt* W9F/N74A/Y140L**

In the W9F/N74A mutant, a CT1 band maximum of 605 nm was observed. In the Y140L single mutant, a CT1 band maximum of 604.5 nm was observed, and in the single mutants W9F and N74A, a CT1 band of 608.5 nm and 607.5 nm were observed, respectively. In order to find out whether or not W9 or N74 could donate any hydrogen bonds to bound fluoride, the triple mutant W9F/N74A/Y140L was made. A CT1 band maximum of 606nm was observed. This result is surprising at first glance - a lack of hydrogen-bonding in the distal heme pocket being donated to bound fluoride should lead to a blue, rather than a red shift. The triple mutant represents a red shift with respect to Y140L. While a CT1 band of at most 604.5 was expected, it should be noted that this triple mutant opens up a lot of space in the distal heme pocket. For each mutation ( $W \rightarrow F$ ,  $N \rightarrow A$  and  $Y \rightarrow L$ ), additional space in the heme pocket is available that is not normally there. In the  $Fe^{3+}$  form, *Tt* H-NOX has a water bound when not in the presence of competing anions. As a result, it is entirely possible that water is staying in the heme pocket after fluoride binds and hydrogen-bonding to bound fluoride. This would account for the red shift with respect to the Y140L mutant. This would also make sense because while the water may hydrogen bond to the bound fluoride, the protein did not evolve to have water play this role, which explains why the CT1 band in the triple mutant is still blue-shifted with respect to

WT. The opening of so much space in the distal heme pocket could also explain the high  $K_{D(F^-)}$ . The  $K_{D(F^-)}$  was measured to be  $374.52 \pm 34.01$  mM in the triple mutant, suggesting that the changes in this mutant are farther-reaching than just the hydrogen-bonding network of the distal heme pocket, affecting other protein structures. Another explanation for the high  $K_{D(F^-)}$  is that in the Y140L mutant, both W9 and N74 shift slightly and stabilize the fluoride. In the W9F/N74A/Y140L mutant, this cannot occur, so fluoride binds much less tightly.

**Adding hydrogen-bond stabilization to bound ligand decreases Fe-F bond strength;  
decreasing hydrogen-bond stabilization to bound ligand increases Fe-F bond strength**

We now show a clear link between ligand polarity as affected by changes to the hydrogen-bonding network in the distal heme pocket of *Tt* H-NOX. The hydrogen-bonding network in the distal heme pocket of *Tt* H-NOX clearly has a relation to the CT1 band maxima (Figure 3). In doing this, we have confirmed that the assay by which fluoride is used as a sensitive probe of distal heme pocket hydrogen bonding is more broadly applicable (17).

Our data indicate that in *Tt* H-NOX, increasing hydrogen-bond stabilization to bound fluoride decreases the Fe-F bond strength. In the F78Y mutant, we see a CT1 band maximum of 618 nm, 9 nm higher than that of WT. Because the CT1 band is a measure of the state of ligand polarity as a result of its interaction with heme iron, we are confident that the F78Y mutant is indeed donating an additional hydrogen bond to fluoride. Additionally, our data shows that decreasing the amount of hydrogen-bonding available to fluoride increases the Fe-F bond strength. Our data shows that Y140 acts as a stabilizer for bound fluoride. This result agrees

with previous studies, which showed that Y140 is responsible for O<sub>2</sub> binding in *Tt* H-NOX in its ferrous state (14).

By the same logic as previously mentioned, the Y140L mutants CT1 band of 604.5 nm indicates that the Fe-F bond is stronger. This fits in well because Y140 is no longer there to donate a hydrogen bond to fluoride. Furthermore, our W9F and N74A single mutants, as well as the W9F/N74A double mutant confirm that decreasing hydrogen bond donation to bound fluoride decreases the CT1 band maximum.

We have also shown a correlation between the strength of hydrogen-bonding to bound ligand and the  $K_{D(F^-)}$ . In general, when there is less hydrogen-bond stabilization afforded to the bound fluoride, the  $K_{D(F^-)}$  increases. Our F78Y, F78Y/Y140L and W9F/N74A/Y140L mutant are predicted to cause additional changes to the heme pocket, explaining their high  $K_{D(F^-)}$  values.

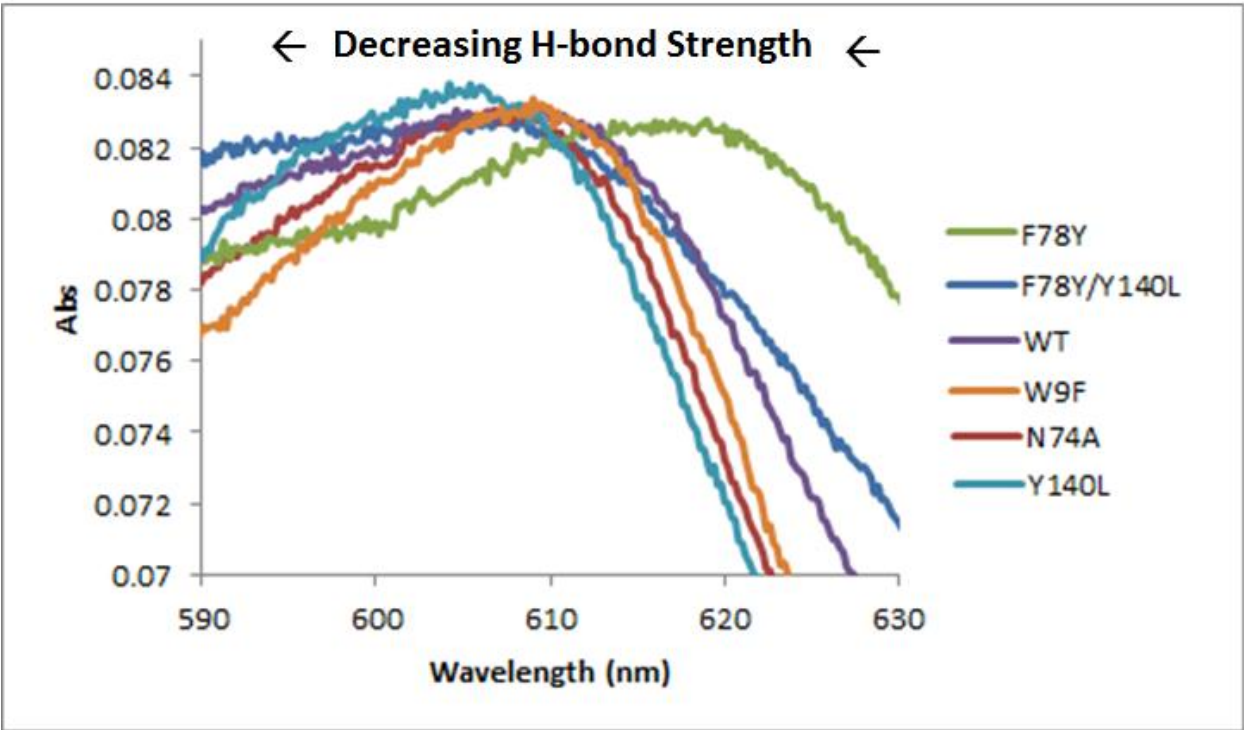


Figure 2-3. The CT1 band maximum blue shifts as hydrogen-bond stabilization of bound fluoride decreases.

## 2.7 Conclusions

We have shown that the CT1 band maxima in *Tt* H-NOX correlates to the strength of hydrogen bonding being donated to bound fluoride by UV-VIS spectroscopy based on the changing the strength of the Fe-F bond. In doing this, we have demonstrated that Y140 is the predominant hydrogen bonding force as an anion-stabilizing residue. We have also shown in the F78Y mutant that destabilizing the Fe-F bond by adding an extra hydrogen bond causes the CT1 to red shift, in line with our other CT1 band data. However, the unexpectedly high  $K_{D(F^-)}$  of the F78Y mutant suggests that sterics may be influencing fluoride stabilization. We find that N74 plays a much larger fluoride stabilization role with respect to Y140 than does W9, as evidenced by spectral properties resembling WT in the W9F mutant. The W9F/N74A mutant displays spectral properties similar to the Y140L mutant, confirming that W9 does in fact stabilize Y140. Our studies also show that the  $K_{D(F^-)}$  is related to the amount of hydrogen-bond stabilization of bound fluoride. When there is more hydrogen-bond stabilization of fluoride, the  $K_{D(F^-)}$  decreases, and when there is less hydrogen-bond stabilization of fluoride,  $K_{D(F^-)}$  increases.

## **Chapter 3: Investigations into the relationship between heme planarity and function in *Tt* H-NOX**

### **3.1 Abstract**

The structure of the heme cofactor is critical for hemoprotein function. These functions include transportation and storage of diatomic gases, chemical catalysis, diatomic gas detection, and electron transfer. In *Tt* H-NOX WT, the heme has been shown to be distorted, due to a proline in the 115 position. In order to investigate the nature of the non-planar heme in H-NOX, we created a panel of mutant *Tt* H-NOX proteins, in which the proline in position 115 was mutated to various residues (P115G, P115A, P115L, P115V, P115W and P115F). At the conclusion of this work we were unable to find a link between heme planarity and redox potential or ligand stabilization by hydrogen-bonding. However, we are undertaking further studies to reach this goal.

### 3.2 Introduction

The H-NOX (Heme Nitrogen and/or OXygen binding) domain from the anaerobe *Thermoanaerobacter tengcongensis* (*Tt*) has the most distorted protein-bound heme group characterized to date. While specific residues in the heme pocket play an obvious role in heme-bound ligand stabilization (14), heme planarity may play a role in ligand stabilization by altering the hydrogen-bonding environment in the distal heme pocket. Using the same detection method described earlier (fluoride in combination with CT1 band shifts, as described in chapter 1), here we aim to measure what effect heme planarity has on the relative strength of hydrogen bond stabilization to bound ligand. In addition to changing the hydrogen bonding environment of the distal pocket, we are interested in seeing if heme planarity affects the midpoint redox potential of *Tt* H-NOX.

While no crystal structures exist for the P115V, L, W and F mutants, structures for P115A and WT have been solved. The crystal structure of *Tt* WT shows a distorted heme (for which the proline in residue 115 is responsible) (6). Conversely, the crystal structure of the P115A mutant shows a comparatively flat heme (figure 1-2) (12).

We hypothesize that our panel of P115 mutant proteins (P115G, P115A, P115L, P115V, P115W and P115F) will represent heme conformations whose level of distortion is varied. Heme distortion could have an effect on the position of heme iron with respect to Y140, which could affect the level of hydrogen bond stabilization afforded to bound ligand by Y140. Additionally, we hypothesize that heme deformation will be correlated with heme properties such as redox potential, ligand affinity, spin state, and optical absorption properties. In this

ongoing study, we aim to characterize each P115 heme structure mutant for changes in such properties with the goal of correlating protein-bound heme structure to function.



### 3.3 Materials and Methods

#### Protein expression and purification

Site-directed mutagenesis was carried out as previously described using the Quikchange protocol by lab-mates Zhou Dai and Sandhya Muralidhara by methods described in chapter 1. Proteins were expressed and purified according to previously described protocols as described in chapter 1. Proteins were stored for no longer than two weeks at  $-80^{\circ}\text{C}$  prior to their use.

#### UV-VIS

Proteins to be used in CT1 band measurement were oxidized to their  $\text{Fe}^{3+}$  complexes using 20mM potassium ferricyanide for one hour and desalted on a PD-10 column (GE Healthcare). Samples for CT1 band measurement contained 15-28  $\mu\text{M}$  protein.

#### Redox Potentiometry

Samples for redox potentiometry were left in their isolated  $\text{Fe}^{3+}/\text{Fe}^{2+}$  states and gradually reduced to  $\text{Fe}^{2+}$  by adding small quantities of sodium dithionite. Samples for redox potentiometry contained between 7 and 9  $\mu\text{M}$  protein (7-10 mL volume). The system was deoxygenated for 45 minutes using  $\text{N}_2$  gas flow. Redox titrations were done under active nitrogen gas flow and continuously mixed with a small magnetic stir-bar. The  $\text{Fe}^{2+}$  state of *Tt* H-NOX binds oxygen readily, so keeping a high internal system pressure and ensuring the presence of  $\text{O}_2$  stays at an absolute minimum is necessary. The redox potential measurements were taken using a pH meter set to mV readout. There was a waiting period of approximately five minutes between sodium dithionite additions in order to allow for redox potential readout

stabilization. See figure 3-1 for a pictorial representation of the set-up. Before scanning, the redox potential as indicated by the pH meter set to mV readout was noted along with the scan number. Scanning spanned a range of approximately 500 mV, with the specific measurements depending on the specific mutant being tested. The data was fit to the Nernst equation, with an electron transfer of one.

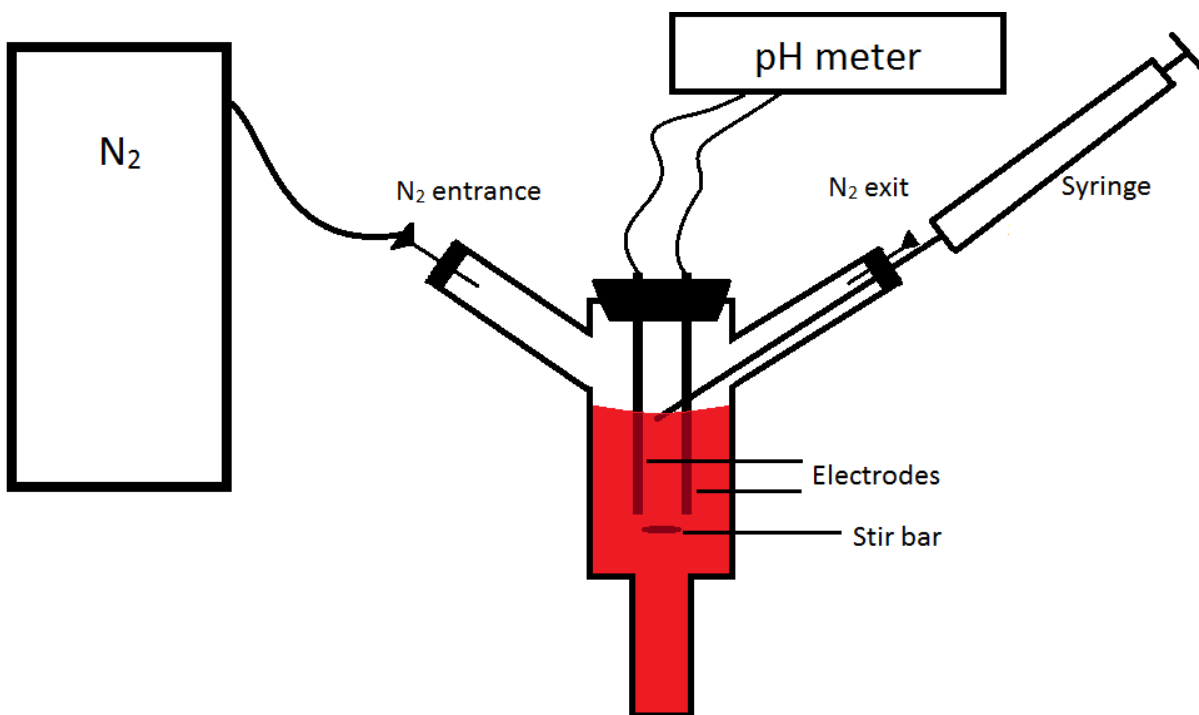


Figure 3-1. Set-up for redox potentiometry. The system is kept at high pressure to ensure no O<sub>2</sub> enters. Sodium dithionite is added through the syringe.

### 3.4 Results and discussion

#### Fluoride as a probe of hydrogen-bonding

The CT1 band maximum of *Tt* H-NOX WT is 609 nm. 609 nm can be used as a reference to which all mutants will be compared.

The CT1 band for P115A is similar to that of wild-type, indicating that no change has been made to the hydrogen bond length from hydrogen bond length from Y140 to bound fluoride. This could be due to the nature of the heme change. The heme is flat in the P115A mutant and distorted in the WT protein, but when looking at the alignment of P115A and WT heme, it is clear that the heme iron has not moved as much as other parts of the heme (Iron moved 0.6 angstroms, while other parts of the heme have moved as much as 1.7 angstroms) (6).

The CT1 band of P115G is similar to that of wild-type, indicating that no change has been made to the hydrogen bond length from hydrogen bond length from Y140 to bound fluoride. The case of P115G may be similar to that of P115A: while the heme may be more flat in the P115G mutant than in WT, the heme iron may not have shifted appreciably.

The CT1 band of P115L is 1.5nm less than that of wild-type, indicating that the length of the hydrogen bond donated from Y140 to bound fluoride may have increased, leading to a weakening of hydrogen bond stabilization. Due to leucine having a rather long R group, sterics may be causing the heme-bound histidine in position 102 to be pushed, moving the heme away

from Y140. This could result in weaker hydrogen bond stabilization, accounting for the CT1 band blue shift.

The CT1 band for P115F is two nm less than wild-type, indicating that the length of the hydrogen bond donated from Y140 to bound fluoride may have increased further than that of the P115L mutant, leading to an even greater weakening of hydrogen bond stabilization. Similar to P115L, steric bulk may be pushing the heme-bound histidine in position 102, causing the heme to be moved away from Y140. Furthermore, because phenylalanine is larger than leucine, this result falls in line with the sterics of phenylalanine pushing the heme further than leucine would, resulting in a greater CT1 band shift.

The P115V mutant having a CT1 band maxima of  $606.4 \pm 0.2$ nm indicates that the hydrogen bond stabilization to bound fluoride is decreasing, leading to a stronger Fe-F bond. We are not currently sure how the P115V mutant results in a CT1 band shift greater than P115L and P115F. It appears that the P115V mutant causes a rather large movement of the heme group, or by some other mechanism is weakening hydrogen bonding from Y140. Additional studies currently being undertaken may elute a rational explanation.

In P115W, the hydrogen bonding donated from Y140 seems to have increased significantly. There could be a number of reasons for this. Tryptophan is such a large residue that it could be stacking with the heme or otherwise displacing it in such a way that causes it to be pushed up into the distal pocket, closer to Y140, decreasing the length of the hydrogen bond being donated to bound fluoride. This could have the effect of increasing the stabilization of

bound fluoride by Y140. This would weaken the Fe-F bond, as shown by a red shift in the CT1 band.

| Protein | CT1 band absorbance maximum (nm) | Midpoint Redox Potential (mV) |
|---------|----------------------------------|-------------------------------|
| WT      | 609 ± 0.2                        | 141.5                         |
| P115A   | 609 ± 0.2                        | 53.2 ± 0.1                    |
| P115G   | 609 ± 0.2                        | 26.6 ± 8.9                    |
| P115L   | 607.5 ± 0.2                      | 14.0 ± 0.6                    |
| P115F   | 607 ± 0.2                        | 41.0 ± 3.5                    |
| P115V   | 606.4 ± 0.2                      | -15.1 ± 5.1                   |
| P115W   | 611 ± 0.2                        | -74.7 ± 5.1                   |

Table 3-1. CT1 band absorbance maximum and midpoint redox potential values. Errors were determined by averaging data.

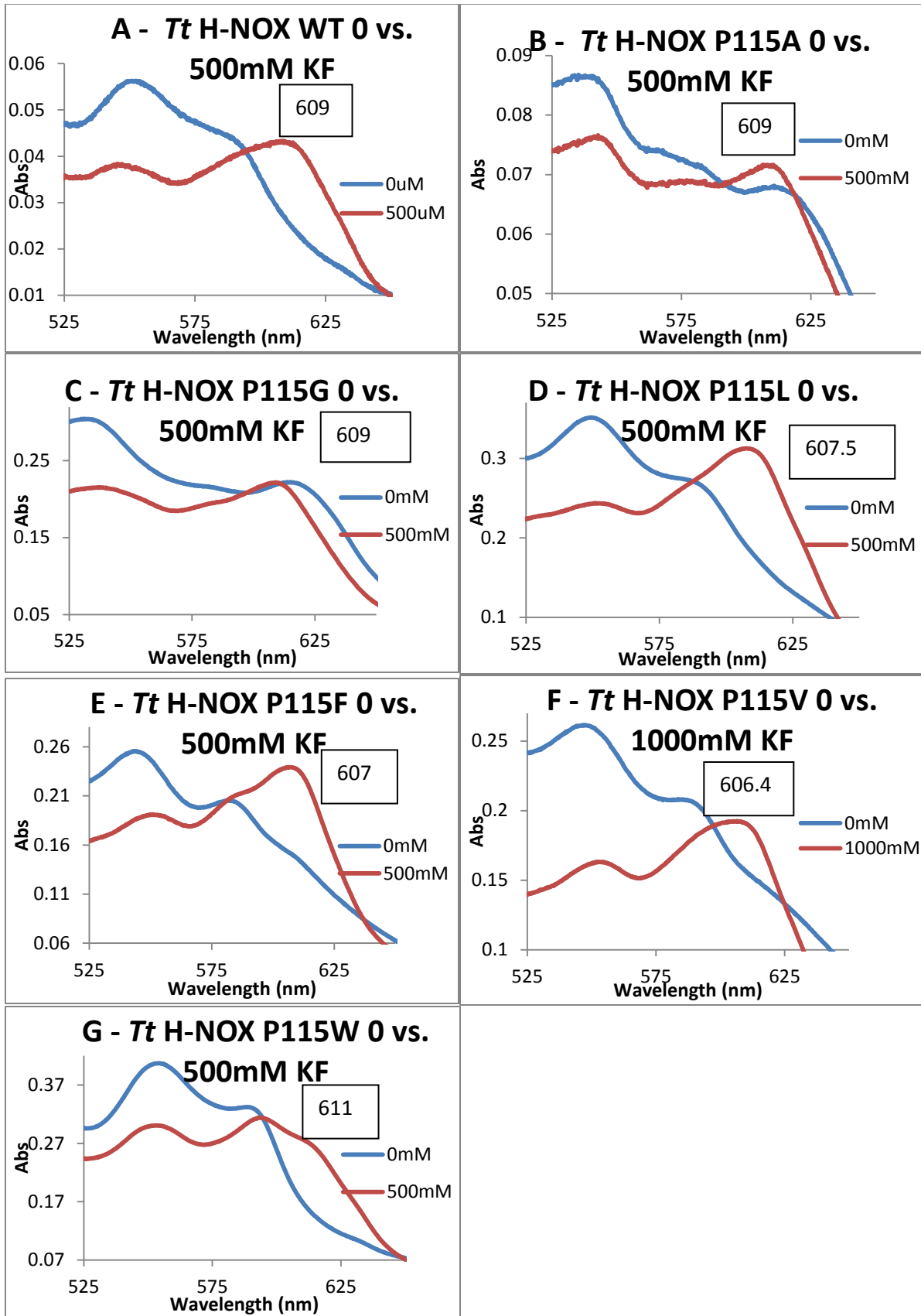


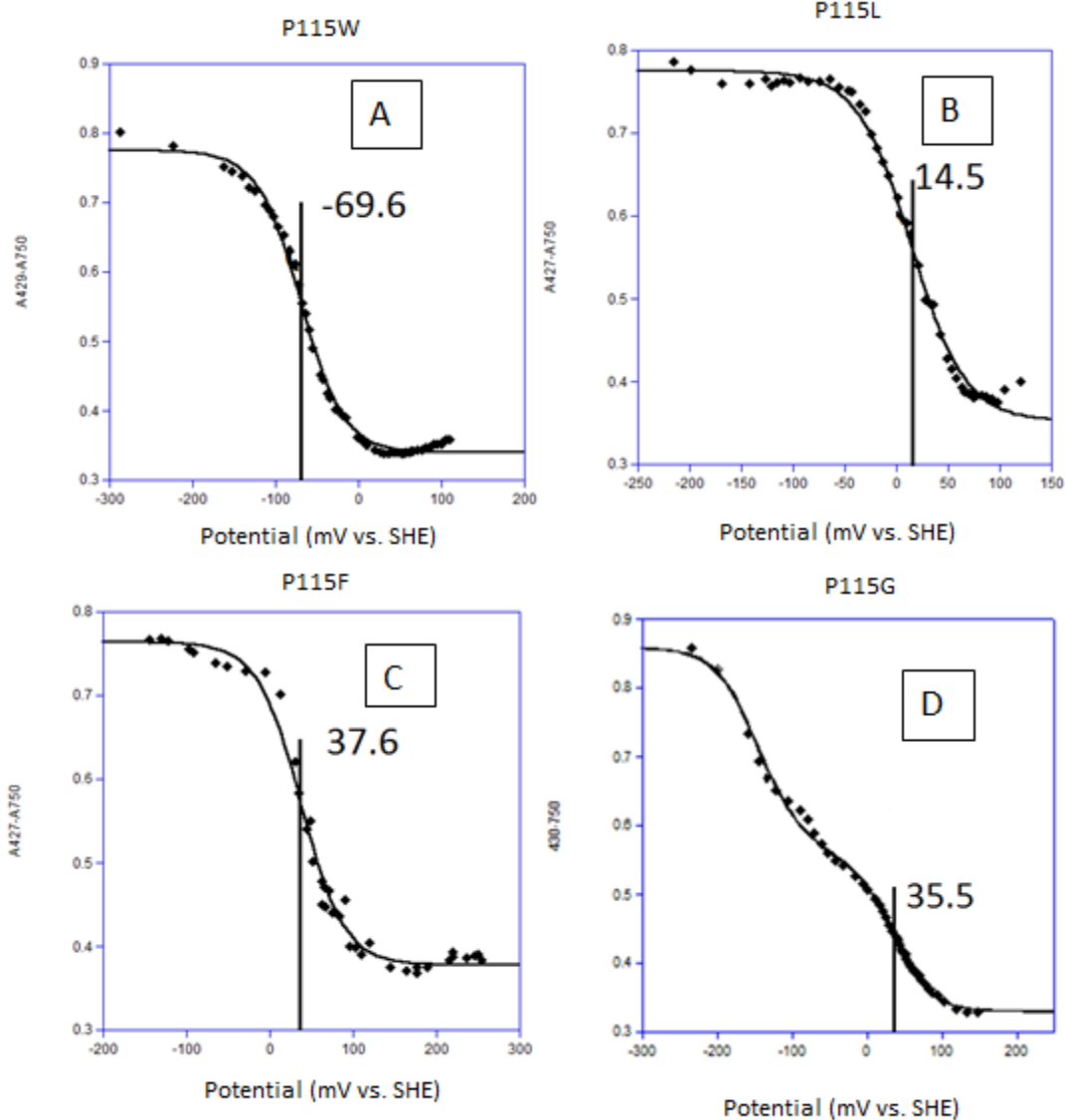
Figure 3-2. The CT1 band of *Tt* P115X mutants. A) WT,  $609 \pm 0.2$  nm. B) P115A,  $609 \pm 0.2$  nm. C) P115G,  $609 \pm 0.2$  nm. D) P115L,  $607.5 \pm 0.2$  nm. E) P115F,  $607 \pm 0.2$  nm. F) P115V,  $606.4 \pm 0.2$  nm. G) P115W,  $611 \pm 0.2$  nm.

### Redox Potentiometry

Free heme has a midpoint redox potential of approximately -220 mV and myoglobin has a midpoint redox potential of approximately 20 mV (19). We measured *Tt* H-NOX WT to have a redox potential of 141 mV. This agrees with previous studies (20). Our measurements also indicate that the P115A mutant has a redox potential of  $53.2 \pm 0.1$  mV. We hypothesized that the midpoint redox potential of our panel of mutants would be correlated to the level of heme distortion present in any given mutant. For example, in mild mutations, such as P115F and P115V, we were expecting values in between those of WT and the P115A mutant, which would represent varying levels of heme distortion. We also expected mutants such as P115W and P115G to display interesting midpoint potentials, because they represent drastic changes from P115. *Tt* H-NOX WT and the panel of P115X mutants exhibited midpoint redox potentials that are very different from those of myoglobin and free heme.

What we see is that the midpoint redox potentials do not appear to be related to heme planarity or residue size. In fact, none of the mutants have redox potentials between those of WT and P115A. All measured midpoint potentials are lower than the value for P115A, with P115W being the lowest at  $-74.7 \pm 5.1$  mV. The P115W result is not particularly surprising at first glance, because tryptophan is such a large residue to replace proline with that one would expect a large change. However, P115F, which is also a larger residue than proline, was measured to be  $41.0 \pm 3.5$  mV, while P115G (the smallest residue possible), was measured to be  $26.6 \pm 8.9$  mV. Additionally, P115L was measured to be  $14.0 \pm 0.6$  mV, while P115V was

measured to be  $-15.1 \pm 5.1$  mV. Given these measurements, it is difficult to relate midpoint redox potential to heme planarity, or even residue size. If midpoint redox potential were comparable to residue size, then with the P115W mutant having the largest size and the lowest midpoint redox potential, residues such as P115G should have a redox potential in between those of WT and P115A, which they do not. P115F, which is the second largest residue mutation present, had one of the highest midpoint redox potential.





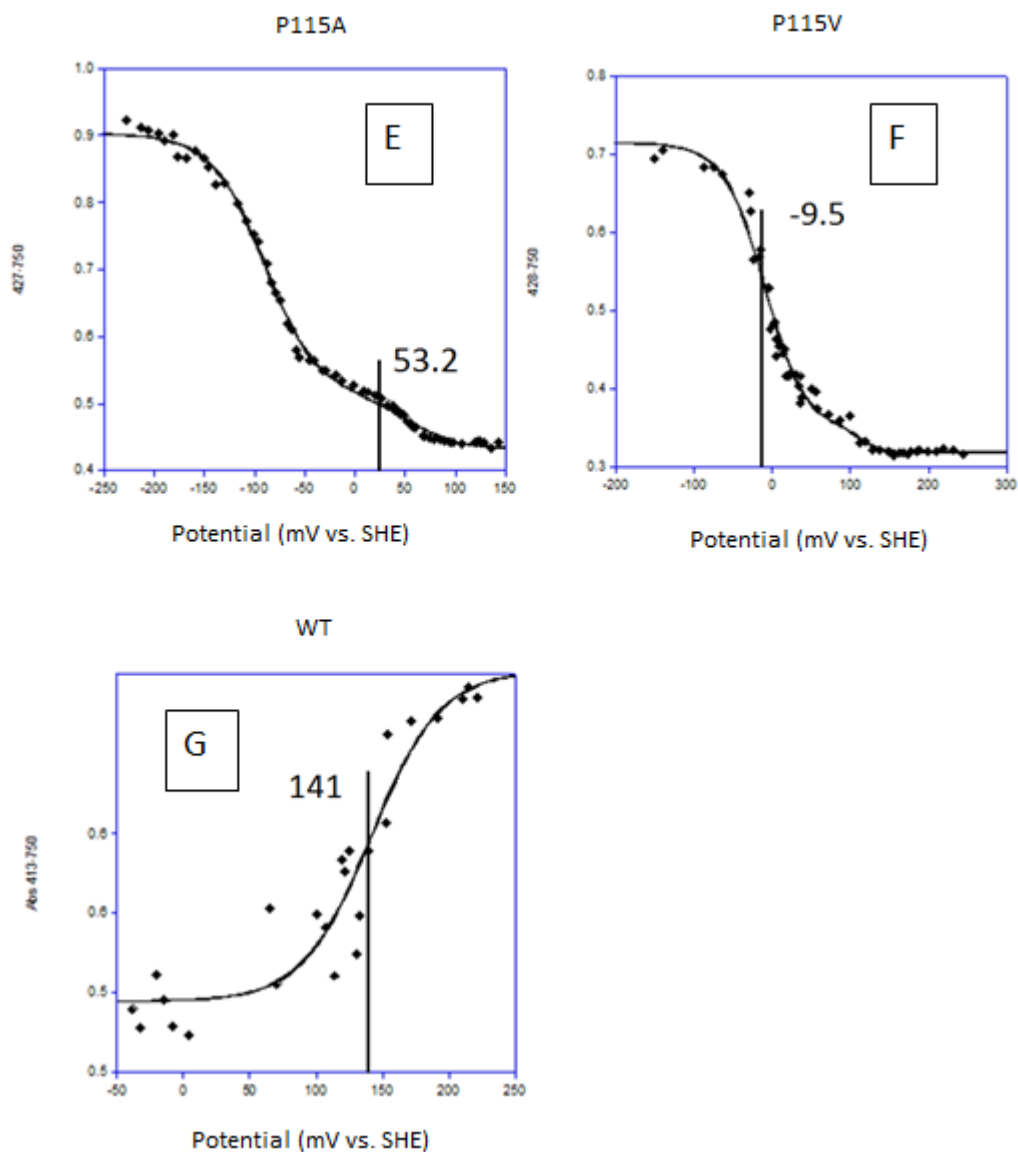


Figure 3-3. Representative redox titrations of *Tt* H-NOX WT and P115X mutants. A) P115W; -69.6 mV. B) P115L; 14.5 mV. C) P115F; 37.6 mV. D) P115G; 35.5 mV. E) P115A, 53.2 mV. F) P115FV; -9.5 mV. G) WT; 141 mV. The Y-axis X-750 refers to the appearance (all mutants, appearance of  $\text{Fe}^{2+}$  species) or disappearance (WT,  $\text{Fe}^{3+}$  species) of a species minus the absorbance at 750 nm. This was then plotted against the potential (mV vs. SHE) as measured for each point.

Although P115G appears to have two redox curves, the spectra shows the presence of only two states, confirming the transfer of only one electron ( $\text{Fe}^{3+} \rightarrow \text{Fe}^{2+}$ ) (appendix A). The P115A mutant also appears to have two redox curves. The P115A mutant appears to have three states, with one at around 387nm. Therefore, the overlap could be due to free heme being reduced. This could be due to free heme in solution (midpoint redox potential has been shown to be -220 mV (19), which would also change the midpoint redox potential. However, if one changes the interpreted midpoint redox potentials of P115A and P115G to the secondary, more negative midpoint, then the midpoint potential for both P115A and P115G is about -90 mV. This measurement coincides with both alanine and glycine being smaller residues, and since the P115A mutant has been shown to have a flat heme (12), it is hypothesized that the P115G mutant also has a flat heme. Therefore, a similar midpoint redox potential in both the P115A and P115G mutants could be related to a flat heme character. Either interpretation puts the midpoint redox potentials of P115A and P115G close together.

### 3.5 Conclusions

Based on our results, we do not see a clear relationship between heme planarity or residue variation and redox potential or hydrogen bond stabilization of fluoride, with the exception that the P115A and P115G residues have similar midpoint redox potentials. Further studies, such as scanning kinetics and x-ray absorption fine structure (XAFS) are being undertaken to try to relate heme planarity and residue variation to function. While we have not yet found a mechanism by which to rationally tune the midpoint redox potential of *Tt* H-NOX, we have shown that varying the residue responsible for heme ruffling in *Tt* H-NOX does have an impact on midpoint redox potential and, to a lesser degree, hydrogen-bond stabilization of bound fluoride.

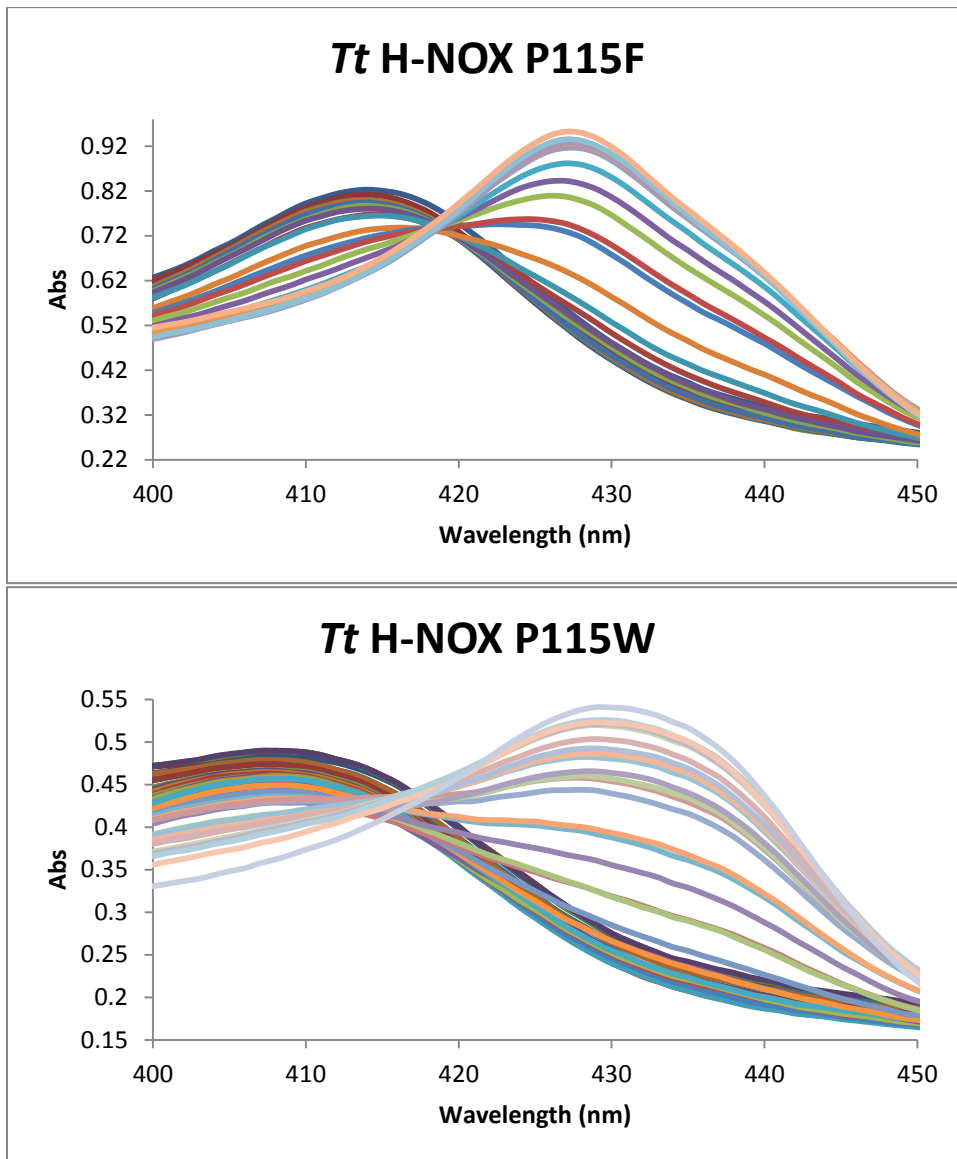
## References

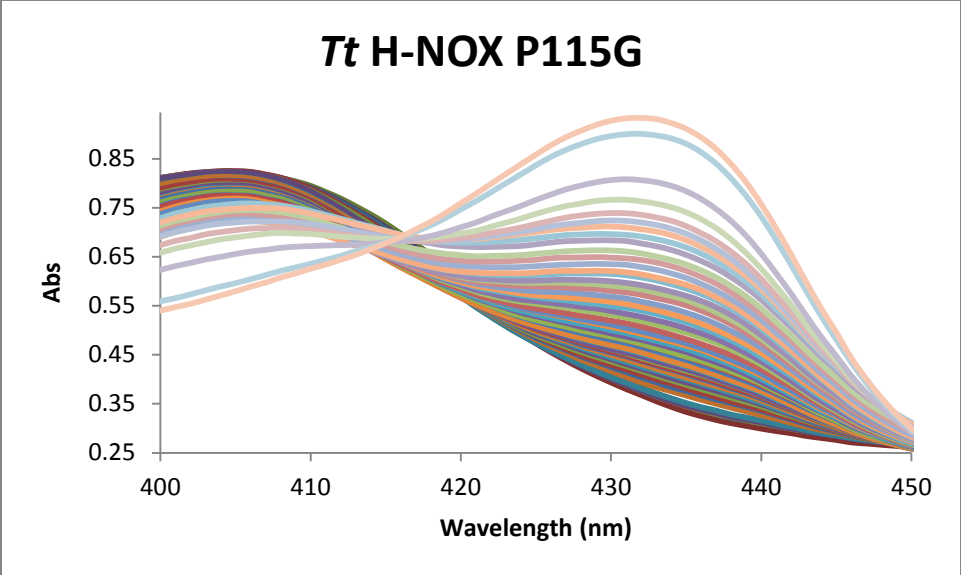
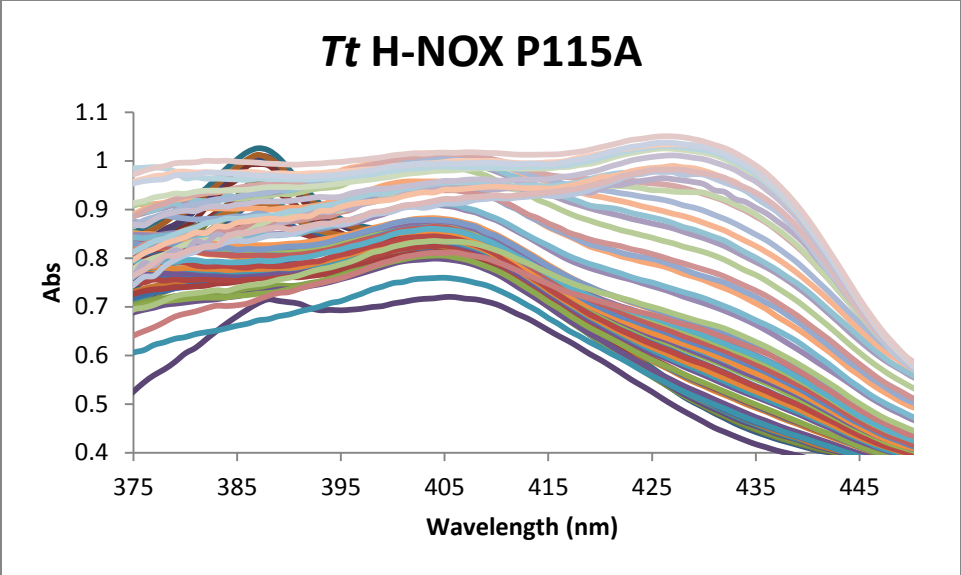
1. Iyer, L. M., Anantharaman, V., and Aravind, L. (2003) Ancient conserved domains shared by animal soluble guanylyl cyclases and bacterial signaling proteins, *BMC genomics* 4, 5.
2. Derbyshire, E. R., and Marletta, M. A. (2009) Biochemistry of soluble guanylate cyclase, *Handbook of experimental pharmacology*, 17-31.
3. Liu, N., Xu, Y., Hossain, S., Huang, N., Coursolle, D., Gralnick, J. A., and Boon, E. M. (2012) Nitric Oxide Regulation of Cyclic di-GMP Synthesis and Hydrolysis in *Shewanella woodyi*, *Biochemistry* 51, 2087-2099.
4. Erbil, W. K., Price, M. S., Wemmer, D. E., and Marletta, M. A. (2009) A structural basis for H-NOX signaling in *Shewanella oneidensis* by trapping a histidine kinase inhibitory conformation, *Proceedings of the National Academy of Sciences of the United States of America* 106, 19753-19760.
5. Henares, B. M., Higgins, K. E., and Boon, E. M. (Submitted) Discovery of a nitric oxide-responsive quorum sensing circuit.
6. Pellicena, P., Karow, D. S., Boon, E. M., Marletta, M. A., and Kuriyan, J. (2004) Crystal structure of an oxygen-binding heme domain related to soluble guanylate cyclases, *Proceedings of the National Academy of Sciences of the United States of America* 101, 12854-12859.
7. Xue, Y., Xu, Y., Liu, Y., Ma, Y., and Zhou, P. (2001) *Thermoanaerobacter tengcongensis* sp. nov., a novel anaerobic, saccharolytic, thermophilic bacterium isolated from a hot spring in Tengcong, China, *International journal of systematic and evolutionary microbiology* 51, 1335-1341.
8. Muralidharan, S., and Boon, E. M. (2012) Heme flattening is sufficient for signal transduction in the H-NOX family, *Journal of the American Chemical Society* 134, 2044-2046.
9. Boon, E. M., and Marletta, M. A. (2005) Ligand specificity of H-NOX domains: from sGC to bacterial NO sensors, *Journal of inorganic biochemistry* 99, 892-902.
10. Olea, C., Jr., Herzik, M. A., Jr., Kuriyan, J., and Marletta, M. A. (2010) Structural insights into the molecular mechanism of H-NOX activation, *Protein science : a publication of the Protein Society* 19, 881-887.
11. Tran, R., Boon, E. M., Marletta, M. A., and Mathies, R. A. (2009) Resonance Raman spectra of an O<sub>2</sub>-binding H-NOX domain reveal heme relaxation upon mutation, *Biochemistry* 48, 8568-8577.
12. Olea, C., Boon, E. M., Pellicena, P., Kuriyan, J., and Marletta, M. A. (2008) Probing the function of heme distortion in the H-NOX family, *ACS chemical biology* 3, 703-710.
13. Dai, Z., and Boon, E. M. (2010) Engineering of the heme pocket of an H-NOX domain for direct cyanide detection and quantification, *Journal of the American Chemical Society* 132, 11496-11503.
14. Boon, E. M., Huang, S. H., and Marletta, M. A. (2005) A molecular basis for NO selectivity in soluble guanylate cyclase, *Nature chemical biology* 1, 53-59.
15. Weinert, E. E., Plate, L., Whited, C. A., Olea, C., Jr., and Marletta, M. A. (2010) Determinants of ligand affinity and heme reactivity in H-NOX domains, *Angew Chem Int Ed Engl* 49, 720-723.
16. Franzen, S., and Boxer, S. G. (1997) On the Origin of Heme Absorption Band Shifts and Associated Protein Structural Relaxation in Myoglobin following Flash Photolysis, *Journal of Biological Chemistry* 272, 9655-9660.
17. Droghetti, E., Nicoletti, F. P., Bonamore, A., Sciamanna, N., Boffi, A., Feis, A., and Smulevich, G. (2011) The optical spectra of fluoride complexes can effectively probe H-bonding interactions in the distal cavity of heme proteins, *Journal of inorganic biochemistry* 105, 1338-1343.

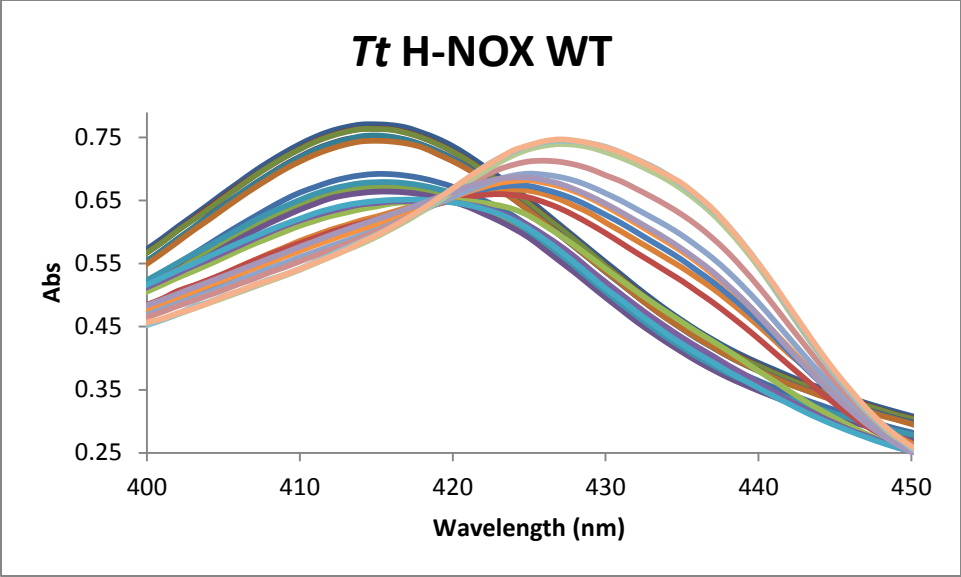
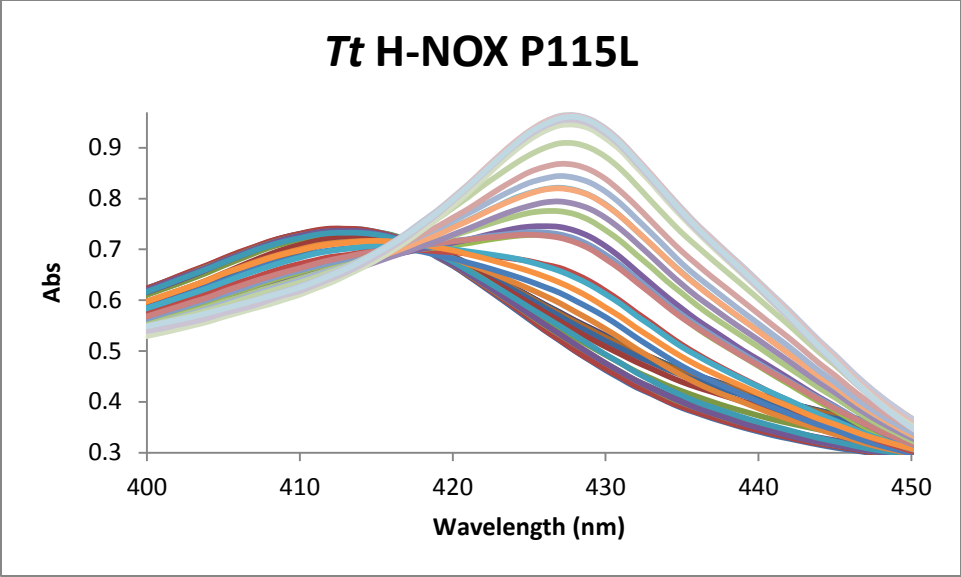
18. Dai, Z., and Boon, E. M. (2011) Probing the local electronic and geometric properties of the heme iron center in a H-NOX domain, *Journal of inorganic biochemistry* 105, 784-792.
19. Moffet, D. A., Foley, J., and Hecht, M. H. (2003) Midpoint reduction potentials and heme binding stoichiometries of de novo proteins from designed combinatorial libraries, *Biophysical Chemistry* 105, 231-239.
20. Olea, C., Kuriyan, J., and Marletta, M. A. (2010) Modulating Heme Redox Potential through Protein-Induced Porphyrin Distortion, *Journal of the American Chemical Society* 132, 12794–12795.

## Appendix A

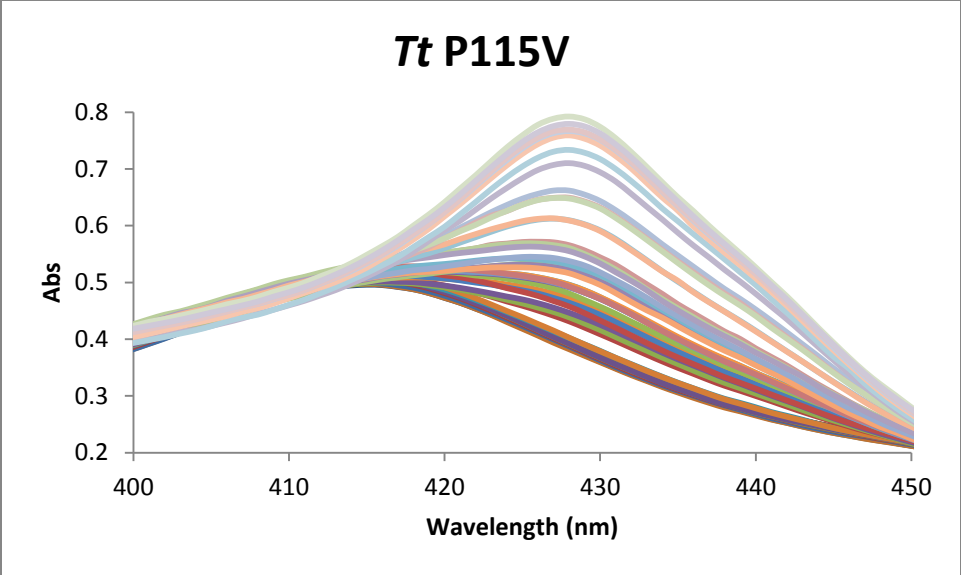
Spectra of *Tt* H-NOX WT and P115X mutants during redox titrations.





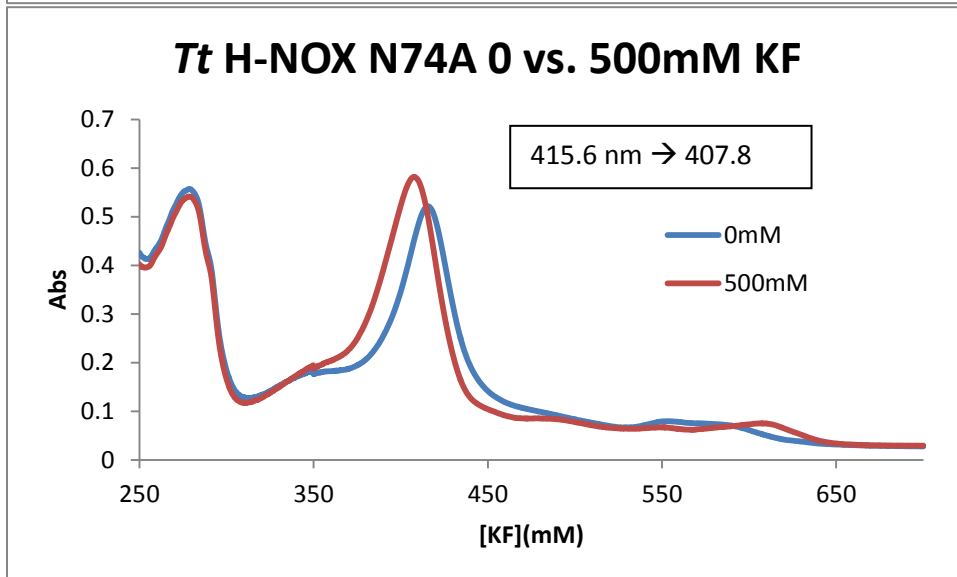
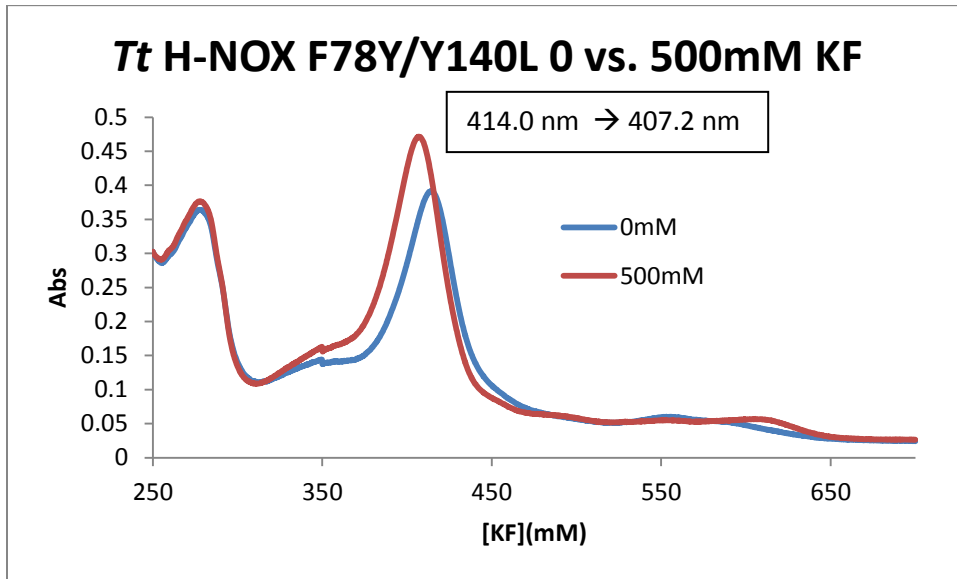




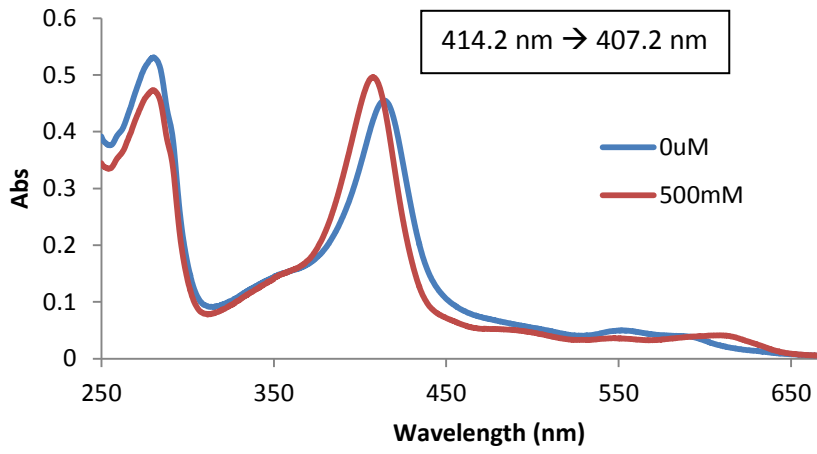


## Appendix B

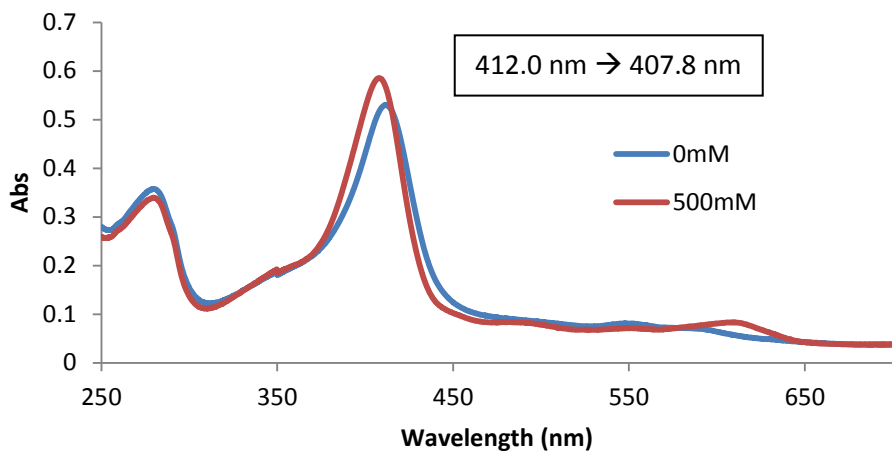
Spectra of characterized proteins.



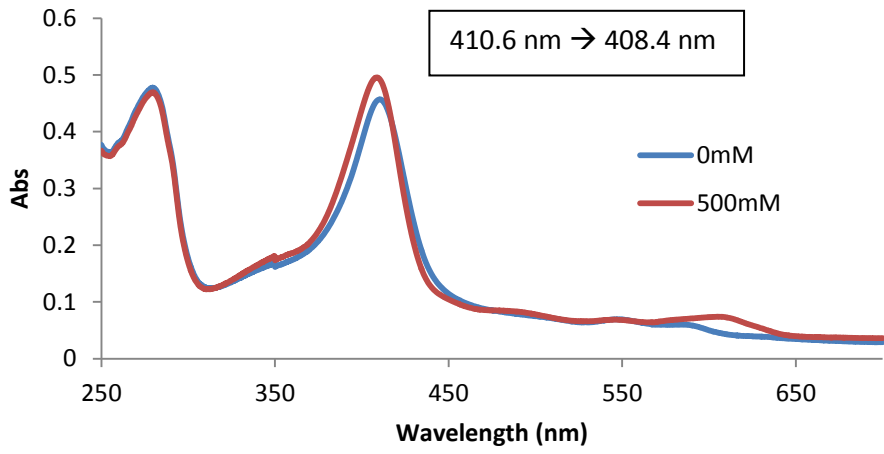
### ***Tt* H-NOX WT 0 vs. 500mM KF**



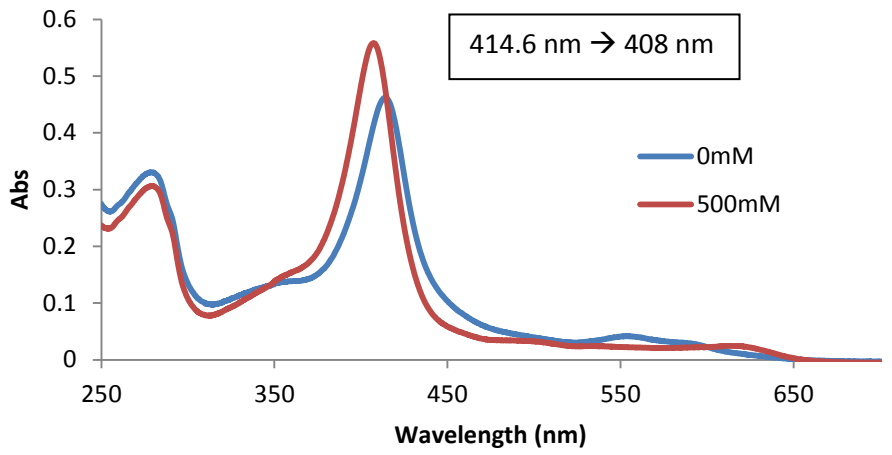
### ***Tt* H-NOX W9F 0 vs. 500 mM KF**



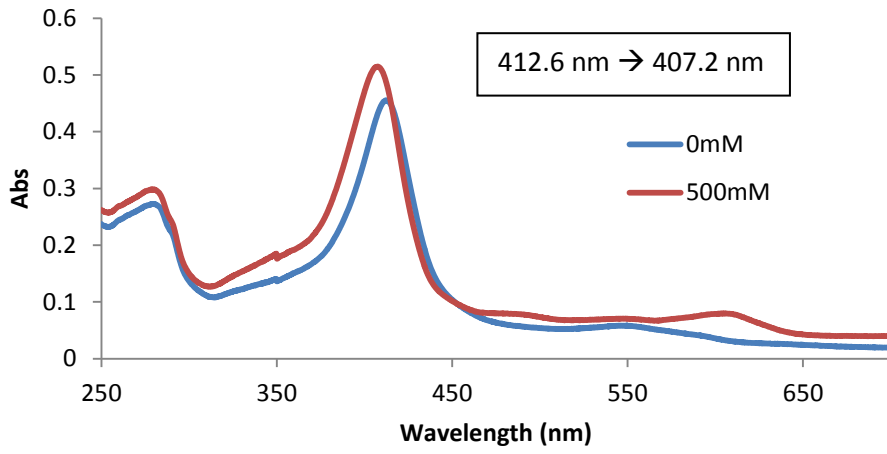
### ***Tt* H-NOX W9F/N74A 0 vs. 500mM KF**



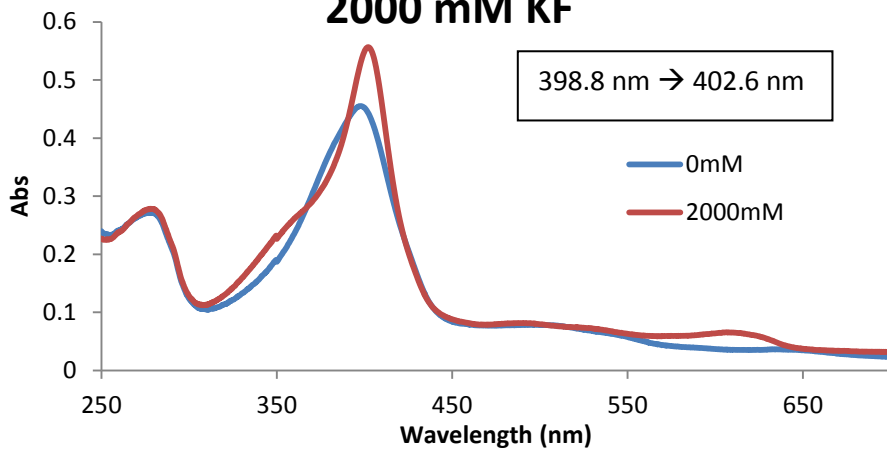
### ***Tt* H-NOX F78Y 0 vs. 500mM KF**



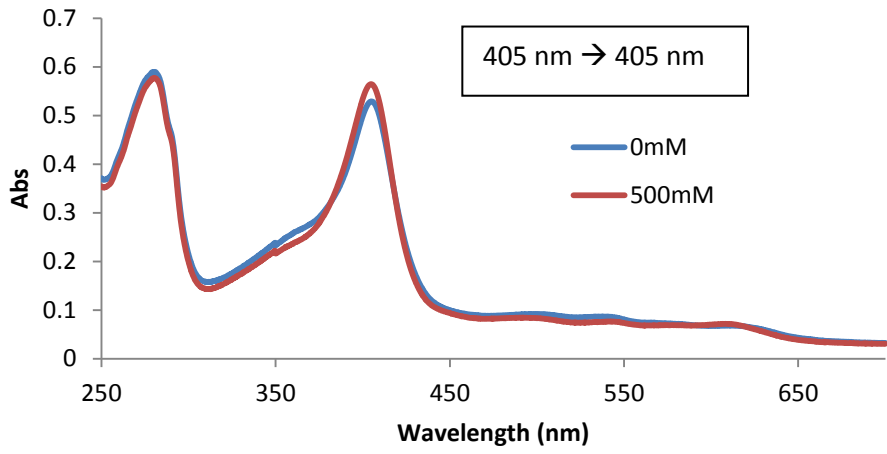
### ***Tt* H-NOX Y140L 0 vs. 500 mM**



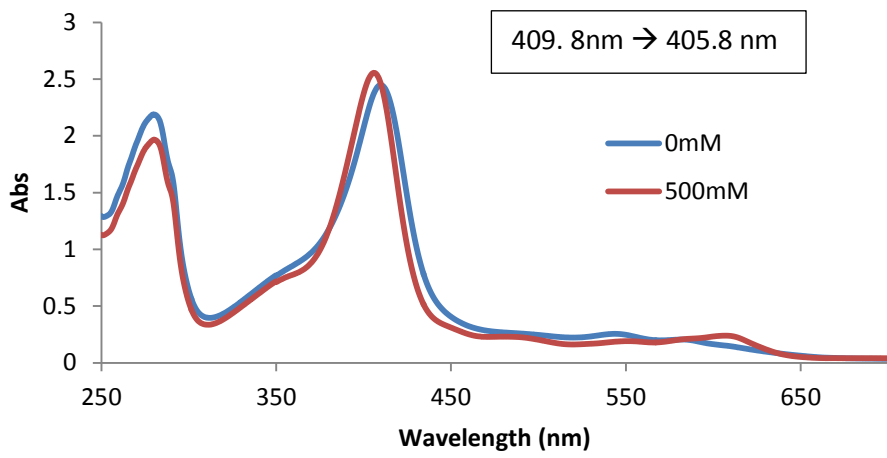
### ***Tt* H-NOX W9F/N74A/Y140L 0 vs. 2000 mM KF**



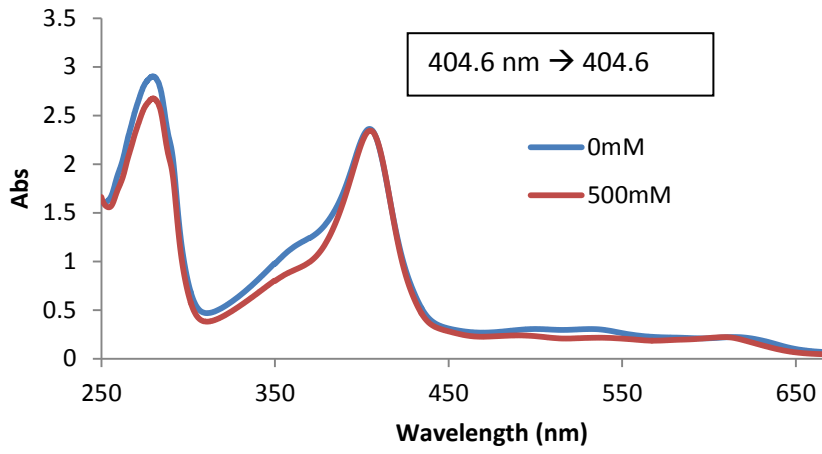
### ***Tt* H-NOX P115A 0 vs. 500mM KF**



### ***Tt* H-NOX P115F 0 vs. 500mM KF**



### ***Tt* H-NOX P115G 0 vs. 500mM KF**



### ***Tt* H-NOX P115L 0 vs. 500mM KF**

